

Review

Cardiovascular Magnetic Resonance Imaging in Ischemic Heart Disease

CME

Florian von Knobelsdorff-Brenkenhoff, MD^{1,2} and Jeanette Schulz-Menger, MD^{1,2*}

This article is accredited as a journal-based CME activity. If you wish to receive credit for this activity, please refer to the website: www.wileyhealthlearning.com

ACCREDITATION AND DESIGNATION STATEMENT

Blackwell Futura Media Services designates this journal-based CME activity for a maximum of 1 *AMA PRA Category 1 CreditTM*. Physicians should only claim credit commensurate with the extent of their participation in the activity.

Blackwell Futura Media Services is accredited by the Accreditation Council for Continuing Medical Education to provide continuing medical education for physicians.

EDUCATIONAL OBJECTIVES

Upon completion of this educational activity, participants will be better able to describe the various applications of CMR for the assessment of ischemic heart disease from a clinical perspective.

ACTIVITY DISCLOSURES

No commercial support has been accepted related to the development or publication of this activity.

Faculty Disclosures:

The following contributors have no conflicts of interest to disclose:

Editor-in-Chief: C. Leon Partain, MD, PhD

CME Editor: Scott B. Reeder, MD, PhD

CME Committee: Scott Nagle, MD, PhD, Pratik Mukherjee, MD, PhD, Shreyas Vasanawala, MD, PhD, Bonnie Joe, MD, PhD, Tim Leiner, MD, PhD, Sabine Weckbach, MD, Frank Korosec, PhD

Authors: Florian von Knobelsdorff-Brenkenhoff, MD, Jeanette Schulz-Menger, MD

This manuscript underwent peer review in line with the standards of editorial integrity and publication ethics maintained by *Journal of Magnetic Resonance Imaging*.

The peer reviewers have no relevant financial relationships. The peer review process for *Journal of Magnetic Resonance Imaging* is double-blinded. As such, the identities of the reviewers are not disclosed in line with the standard accepted practices of medical journal peer review.

Conflicts of interest have been identified and resolved in accordance with Blackwell Futura Media Services's Policy on Activity Disclosure and Conflict of Interest. No relevant financial relationships exist for any individual in control of the content and therefore there were no conflicts to resolve.

INSTRUCTIONS ON RECEIVING CREDIT

For information on applicability and acceptance of CME credit for this activity, please consult your professional licensing board.

This activity is designed to be completed within an hour; physicians should claim only those credits that reflect the time actually spent in the activity. To successfully earn credit, participants must complete the activity during the valid credit period.

Follow these steps to earn credit:

- Log on to www.wileyhealthlearning.com
- Read the target audience, educational objectives, and activity disclosures.
- Read the article in print or online format.
- Reflect on the article.
- Access the CME Exam, and choose the best answer to each question.
- Complete the required evaluation component of the activity.

This activity will be available for CME credit for twelve months following its publication date. At that time, it will be reviewed and potentially updated and extended for an additional period.

¹Working Group on Cardiovascular Magnetic Resonance, Medical University Berlin, Experimental Clinical Research Center, a joint cooperation of the Charité and the Max-Delbrück-Center, Berlin, Germany.

²HELIOS Klinikum Berlin-Buch, Department of Cardiology and Nephrology, Berlin, Germany.
Contract grant sponsor: Else Kröner Fresenius-Stiftung.

*Address reprint requests to: J.S.-M., Working Group on Cardiovascular Magnetic Resonance, Medical University Berlin, Charité Campus Buch, Experimental and Clinical Research Center and HELIOS Klinikum Berlin-Buch, Department of Cardiology and Nephrology, Schwanebecker Chaussee 50, 13125 Berlin, Germany. E-mail: jeanette.schulz-menger@charite.de

Received March 22, 2011; Accepted December 9, 2011.

DOI 10.1002/jmri.23580

View this article online at wileyonlinelibrary.com.

Ischemic heart disease is the most frequent etiology for cardiovascular morbidity and mortality. Early detection and accurate monitoring are essential to guide optimal patient treatment and assess the individual's prognosis. In this regard, cardiovascular magnetic resonance (CMR), which entered the arena of noninvasive cardiovascular imaging over the past two decades, became a very important imaging modality, mainly due to its unique versatility. CMR has proven accuracy and is a robust technique for the assessment of myocardial function both at rest and during stress. It also allows stress perfusion analysis with high spatial and temporal resolution, and provides a means by which to differentiate tissue such as distinguishing between reversibly and irreversibly injured myocardium. In particular, the latter aspect is a unique benefit of CMR compared with other noninvasive imaging modalities such as echocardiography and nuclear medicine, and provides novel information concerning the presence, size, transmurality, and prognosis of myocardial infarction. This article is intended to provide the reader with an overview of the various applications of CMR for the assessment of ischemic heart disease from a clinical perspective.

Key Words: magnetic resonance; acute coronary syndrome; chronic coronary artery disease; stress test

J. Magn. Reson. Imaging 2012;36:20–38.

© 2012 Wiley Periodicals, Inc.

CORONARY ARTERY DISEASE (CAD), almost exclusively caused by atherosclerosis, is the leading cause of death in developed countries (1). From a clinical point of view, CAD can either present acutely during acute myocardial infarction (MI), or chronically, potentially ending up in ischemic cardiomyopathy with heart failure, arrhythmias and ischemic valvular disease. Despite general medical progress, there is concern that the predominance of cardiovascular mortality will even increase in future considering the growing prevalence of obesity and diabetes and poorly controlled additional risk factors for cardiovascular disease (2). Therefore, prevention, early detection and accurate characterization of CAD are strongly warranted to allow for effective prophylactic strategies and to optimally guide therapies, both for the individual's sake, and for the cost burden of health care systems.

In particular the latter objectives—making the diagnosis of CAD and guiding therapeutic decisions—require excellent diagnostic and imaging tools provided to physicians in clinical medicine. *Cardiovascular magnetic resonance imaging* (CMR) is increasingly applied to examine patients with known or suspected CAD due to its unique diagnostic versatility (3–5). The work-up of CAD was the most frequently named primary indication for performing a CMR study in the EuroCMR registry—45.7% of 11,040 CMR studies (6). CMR provides cine movies of the heart, mostly based on steady-state free-precession acquisitions, with high blood-tissue contrast to allow for accurate cardiac chamber quantification and wall motion analysis both at rest and at stress (7). It enables myocardial perfusion studies to detect myocardial ischemia (8), and gives insights into the morphology of the myocardial tissue (9) (Table 1). The latter characteristic ena-

bles to noninvasively differentiate various causes of myocardial injury—like ischemia or inflammation—various stages of myocardial injury—like acute and chronic—and various severity grades of myocardial cell damage—like reversible and irreversible.

This review is intended to give an overview over the applications and role of CMR in the work-up of patients with known or suspected CAD. While the article focuses on the clinical point of view, some technical aspects are also mentioned, and future trends are touched.

ASSESSMENT OF MYOCARDIAL ISCHEMIA: CMR STRESS TESTS

A stress test is often indicated in symptomatic patients with typical or atypical chest pain or correlates suspected of being due to CAD and who have a low or intermediate cardiovascular risk profile, as well as in asymptomatic patients with high cardiovascular risk profiles, such as diabetics, or in patients with known CAD during follow-up (10). Exercise electrocardiography (ECG) is usually the first-level stress test, but this may not be appropriate for some patients (e.g., those with limited physical capacity) or nondiagnostic (e.g., due to not reaching the target heart rate). Therefore, stress tests that include noninvasive imaging are frequently used. Left ventricular wall-motion abnormalities induced by stress can be assessed both by using CMR and transthoracic echocardiography (TTE). Furthermore, myocardial perfusion analysis during stress is possible if using CMR or single photon emission computed tomography (SPECT).

All methods have strengths and weaknesses, and it would be beyond the scope of the present article to provide a comprehensive review of all available methods. To date, there are no studies that have compared all approaches to identify the test modality with the best diagnostic accuracy. However, in general when assessing and comparing the diagnostic accuracy of various procedures, it should be kept in mind that the underlying gold standards often differ between studies: although usually invasive coronary angiography is selected for comparison, the threshold of a relevant coronary artery stenosis varies in published studies. Furthermore, the significance of the different target parameters of the various diagnostic tests—anatomy of stenosis versus wall motion abnormality versus perfusion defect—must be taken into account when comparing diagnostic procedures. For example, there might be a high-grade stenosis detected by invasive coronary angiography, but no perfusion defect or wall motion abnormality by CMR stress tests. Such a constellation would, therefore, reduce the sensitivity of CMR tests when defining angiography as the gold standard. Rather, the techniques have to be interpreted as complementary, with CMR expressing the hemodynamic relevance of an anatomic stenosis (11). Similarly, CMR stress perfusion might reveal a subendocardial perfusion defect, whereas coronary angiography excludes any stenosis of the epicardial coronary arteries. This might be interpreted as reflecting a low

Table 1
CMR Modalities Suitable for the Work-up of Ischemic Heart Disease

Example				
CMR modality	Cine imaging (at rest and stress)	T2-weighted imaging	First-pass perfusion imaging (at rest and stress)	Late gadolinium enhancement
Objective	Assessment of cardiac function	Detection of myocardial edema	Assessment of myocardial blood flow	Identification of irreversible myocardial injury
Target parameters	<ul style="list-style-type: none"> • Left ventricular ejection fraction, volumes and mass • Wall motion abnormalities 	<ul style="list-style-type: none"> • Differentiation of acute and chronic infarction • Area at risk • Myocardial salvage • Hemorrhage 	<ul style="list-style-type: none"> • Perfusion defect/Ischemia • Microvascular obstruction 	<ul style="list-style-type: none"> • Infarct size • Viability • Microvascular obstruction • Thrombus

specificity of the CMR test when defining angiography as the gold standard. However, the perfusion defect might in fact be present, and caused by disturbances of the microcirculation. This might provide additional insight into the underlying pathology, such as syndrome x, diabetes, systemic hypertension, or hypertrophic cardiomyopathy (12–14). Therefore, when choosing and evaluating a stress test, the clinician should take the underlying pathophysiology into account.

Cardiac Wall Motion Analysis During Dobutamine Stress

The concept and protocol of dobutamine CMR is similar to dobutamine TTE, and was first introduced approximately 2 decades ago (7,15,16). Left ventricular function is assessed using steady-state free precession (SSFP) cine imaging at rest, and subsequently during increasing dosages of intravenously administered dobutamine—a synthetic beta-1-selective catecholamine agonist—until an age-predicted heart rate response is obtained. If the target heart rate is not reached with the highest dobutamine dosage (usually 40 µg/kg/min), additional fractions of atropine (maximal dose 1mg)—an inhibitor of the vagal tone—is administered intravenously to further stimulate the heart rate. Images are acquired at least in three short axes of the left ventricle, usually with the addition of one or more long axis views as recommended in concordance with the 17-segment model proposed by the American Heart Association (AHA) (17). In the presence of a relevant coronary stenosis, the stress promotes an oxygen supply/demand mismatch that leads to left ventricular wall motion abnormalities (Fig. 1).

However, compared with dobutamine TTE, CMR usually acquires cardiac images only every 3 min, in contrast to the continuous echocardiographic real-time imaging. Furthermore, any analysis of ST-seg-

ment alterations on the ECG indicating ischemia are not feasible during CMR due to distortion of the ECG signal caused by magnetohydrodynamic effects. Nevertheless, significant heart rhythm disorders are

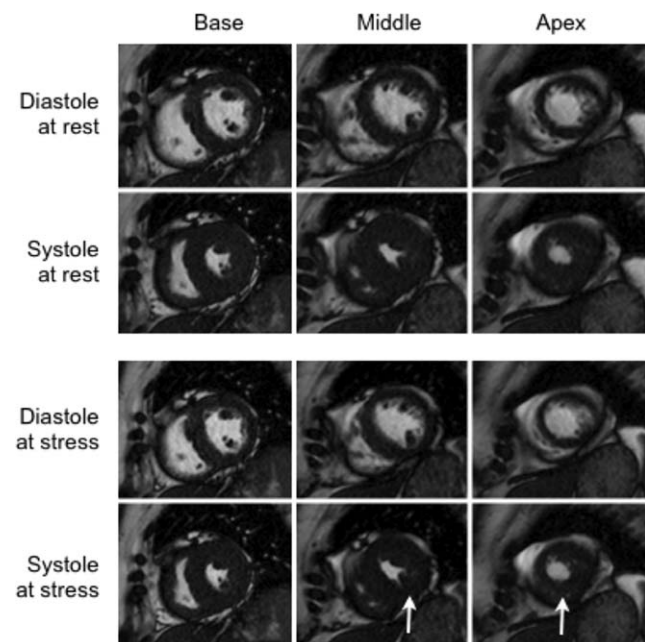


Figure 1. Stress CMR: Wall motion analysis during dobutamine infusion in a 62-year-old woman with three-vessel coronary artery disease and chest pain. The upper panel shows standard short axis views (basal, midventricular, and apical; from left to right), in diastole (top), and systole (bottom) at rest. There is no wall motion abnormality at rest. The lower part of the figure shows the same short axis views during dobutamine infusion at peak heart rate. There is a discrete hypokinesis in the inferior wall indicating a stenosis of the right coronary artery. During subsequent coronary angiography, a stent was implanted into a 75% stenosis of that vessel.

detectable even in the presence of a distorted ECG curve, which makes continuous ECG monitoring mandatory and useful. Under consideration of such safety measures, dobutamine CMR can be performed as safely as dobutamine TTE, with low major adverse event rates of 0.05% to 0.5% (6,18,19), which is comparable to adverse event reports of 0.2% with dobutamine TTE (20).

Overall, the diagnostic accuracy of dobutamine CMR is reported to be superior to dobutamine TTE in cases where there is a reduced ultrasound window. Nagel et al compared the ability to detect a coronary stenosis $\geq 50\%$ as assessed by coronary angiography using dobutamine CMR or dobutamine TTE. They reported a sensitivity of 86% versus 74%, specificity of 86% versus 70%, and diagnostic accuracy of 86% versus 73% (21). Further results underlining the satisfactory diagnostic nature of dobutamine CMR came from Hundley et al, who reported a sensitivity/specifity of 83%/83% (22) for detecting a coronary artery stenosis $\geq 50\%$ as assessed by angiography, and from a meta-analysis by Nandalur et al, who found a sensitivity/specifity of 83%/86%, respectively, to detect a coronary artery stenosis $\geq 50\%$ as assessed by angiography (23). The superiority of CMR compared with TTE is mainly explained by improvements in image quality (21,22). Whereas TTE is dependent on adequate acoustic windows and the proficiency of the sonographers, CMR images can be acquired with good and reproducible image quality independent of the patient's physique and the examiner. The use of standardized procedures for positioning of slices leads to reproducible results and ensures that each slice position can be accurately reproduced at different stress levels. Furthermore, the endocardial border can be clearly delineated because of the high blood/tissue contrast (21). These aspects are particularly important in those patients with wall motion abnormalities even at rest, in whom wall motion interpretation can be very difficult (24). The standardized approach and high image quality likely underlie the documented low interobserver variability and high reproducibility of dobutamine CMR (25,26).

Recent data indicate that the sensitivity of dobutamine CMR for the diagnosis of CAD may be further improved by the addition of first-pass myocardial perfusion imaging to wall motion assessments during peak-dose dobutamine, particularly in patients with left ventricular hypertrophy, in whom the accuracy of dobutamine CMR alone may be reduced (27–29). Furthermore, there are attempts to increase the diagnostic accuracy of dobutamine CMR to detect early evidence of ischemia by supplementing the visual wall motion analysis with quantitative methods like myocardial tissue tagging (30–32). However, because of the need for time-consuming postprocessing, these promising techniques have not yet entered clinical routine. Finally, although most of these diagnostic accuracy data were obtained at 1.5 Tesla (T) field strength, they have also been confirmed for the 3T field strength (33).

While dobutamine CMR to detect myocardial ischemia has important short-term implications to guide re-

vascularization strategies, it has also strong prognostic impact. Hundley et al. found a significant association between dobutamine-induced wall motion abnormalities by CMR and MI, as well as cardiac death (34). Similarly, a normal dobutamine CMR study has been shown to be associated with a very low cardiovascular event rate during the subsequent years, as reported by Kuijpers et al for a 2-year follow-up (35), by Jahnke et al for a 3-year follow-up (36) and recently by Kelle et al for a 6-year follow-up (37).

Myocardial Perfusion Analysis During Vasodilator Stress

Myocardial perfusion imaging by CMR was introduced approximately 2 decades ago (38). Compared with SPECT, which uses a radioisotope that is actively taken up by the myocytes to depict myocardial perfusion, CMR analyzes the first pass of an extracellular contrast agent within the myocardium. Whereas the stress protocol used for both methods is similar, CMR offers the benefit of superior spatial and temporal resolution, and SPECT is associated with the negative effects of exposure to ionizing radiation (8,39).

Myocardial perfusion can be assessed using CMR by acquiring a series of ECG-gated T1-weighted images (using gradient echo, gradient echo-planar, or SSFP acquisitions) (40) with every one to two heart beats during the first pass of an intravenously administered bolus of extravascular contrast media, like gadolinium, during one breath-hold. This is done during simultaneous infusion of a vasodilator, which causes myocardial hyperemia. The predominant vasodilator is adenosine, although dipyridamol is sometimes used. Recently, regadenoson, which is administered as a single bolus and has similar effects on myocardial perfusion as adenosine (41), has been FDA approved for radionuclide perfusion studies. The hyperemic flow is compromised in myocardial segments that are supplied by a significantly stenosed coronary artery because of the drop of coronary perfusion pressure downstream of the coronary stenosis. Alternatively, microvascular dysfunction can lead to an impairment of perfusion reserve despite the absence of any significant stenosis of the epicardial coronary arteries, as mentioned earlier (12–14). Segments with a perfusion defect in relation to the hyperemic myocardium will, therefore, be identifiable by a lower signal intensity on the CMR image (Fig. 2) (8). Images are commonly acquired in at least three short axes of the left ventricle in concordance with the AHA 16-segment model (17); one additional long axis view of the apical segment can be helpful. Early results from studies visualizing the whole heart in three-dimensional (3D) during the stress test are promising (42).

The diagnostic accuracy of stress perfusion CMR has been investigated in several studies. Ishida et al compared the ability to detect $\geq 70\%$ coronary artery stenosis (assessed by angiography) with dipyridamol stress perfusion CMR or SPECT. They found CMR to be superior, with a sensitivity/specifity of 94%/88%

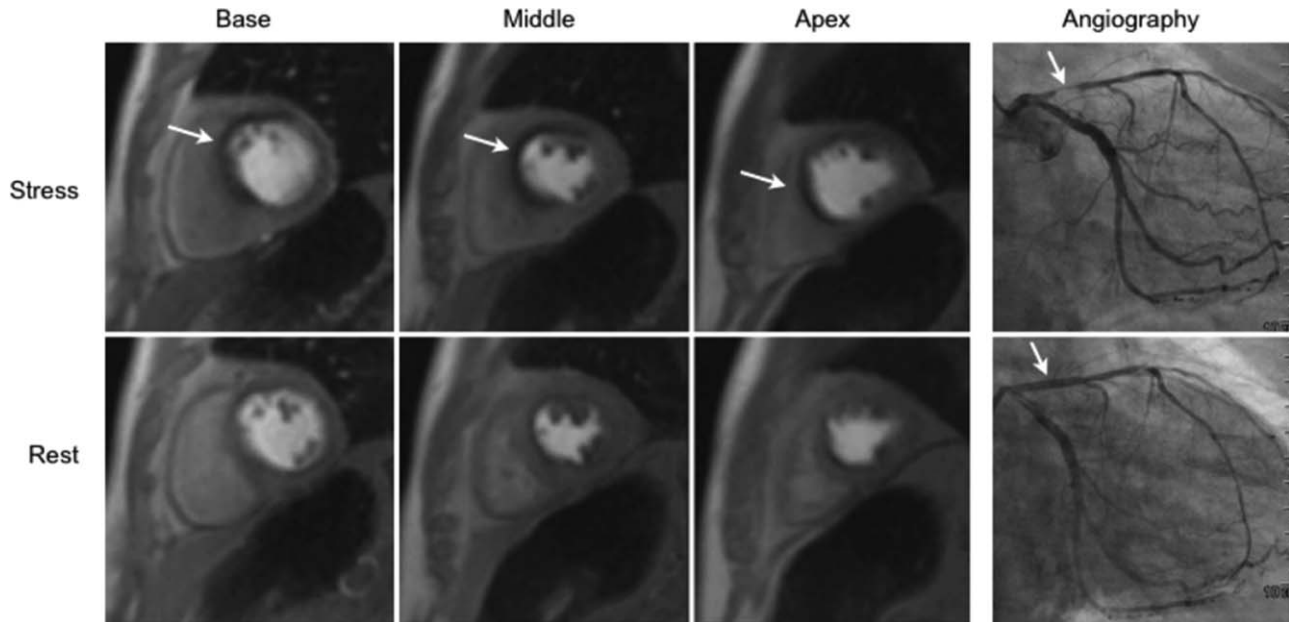


Figure 2. Stress CMR: Myocardial perfusion analysis during vasodilator infusion in a 74-year-old man with chest pain at mild exertion, known two vessel coronary artery disease and no wall motion abnormalities. The top row shows three short axis views (*basal*, *midventricular*, and *apical*) during contrast-enhanced first-pass perfusion CMR during adenosine stress. A large perfusion defect of the anterior and septal wall is obvious (white arrows). The bottom row shows the same slices during contrast-enhanced first-pass perfusion CMR at rest with clearly less extensive perfusion defect. On the right side, the coronary angiography is depicted. A severe stenosis of the proximal left anterior descending artery that supplies the anterior and septal wall is seen (white arrow in the top image). It is treated by stent implantation (white arrow in the bottom image).

versus SPECT with 82%/71%, respectively, on a patient level (43). A randomized multi-center multi-vendor trial (MR-IMPACT), demonstrated that adenosine stress perfusion CMR was equivalent to SPECT at detecting coronary artery stenosis $\geq 50\%$ when assessed by invasive coronary angiography (44). A meta-analysis reported a sensitivity/specification of 91%/81% for the detection of a coronary artery stenosis $\geq 50\%$ (23).

However, when interpreting these results concerning the diagnostic accuracy of CMR stress perfusion, the reader should keep in mind that it is problematic to use single cut-offs like $\geq 50\%$ or $\geq 70\%$ lumen narrowing to define the relevance of a coronary artery stenosis. Apart from variations in stenosis degree depending on the applied quantification technique (45), it is known from pathophysiologic studies that coronary stenosis severity as assessed by coronary angiography does not always correlate with its functional significance in terms of myocardial perfusion (11). Therefore, pressure wire derived fractional flow reserve (FFR) calculation of a coronary stenosis is regarded as the more adequate gold standard to evaluate the diagnostic capability of stress perfusion CMR (46). Using such an approach, Watkins et al found a sensitivity and specificity of stress perfusion CMR for the detection of functionally significant CAD of 91% and 94%, respectively (47); and Lockie et al, who performed FFR and stress perfusion CMR at 3T, recently reported a sensitivity and specificity of 82% and 94% (48).

Most previous studies reporting the diagnostic accuracy of stress perfusion CMR excluded patients with coronary artery bypass grafts in whom there may

be altered myocardial contrast kinetics owing to more complex myocardial perfusion and different distances of the contrast bolus through different bypasses and native coronary vessels. Two recent studies demonstrated that even for patients after surgical revascularization, stress perfusion CMR yields good diagnostic accuracy for the detection and localization of significant stenoses, although the sensitivity is reduced compared with patients without coronary bypass (49,50).

Stress perfusion CMR is regarded as a safe method (6,51). Image analysis can be performed either visually—which is predominantly done in clinical practice, or quantitatively by calculating the rate of myocardial signal change (upslope) during contrast medium first pass—which is predominantly done in research (52,53). Both approaches achieve satisfactory observer dependency, and it is still controversial whether any approach is superior (48,54).

The step from 1.5T to 3T leads to a significant increase in myocardial signal during the first pass of contrast media (55), which leads to improved image quality and fewer extended dark rim artifacts. However, whether these benefits can also be translated into superior diagnostic accuracy is still under debate (56,57). Similarly, promising efforts to increase temporal and spatial resolution by integrating modern acceleration methods during image reconstruction can be conducted (58). However, evidence of their impact on diagnostic accuracy remains to be determined.

In addition to its important short-term use to guide revascularization strategies, stress perfusion CMR

also has a strong prognostic impact. Steel et al. reported that a perfusion defect on CMR was associated with a three-fold increase in risk of cardiac death or acute MI in patients referred with symptoms of myocardial ischemia during a median follow-up of 17 months (59). Ingkanisorn et al demonstrated in patients with chest pain, who had MI excluded by blood tests and nondiagnostic ECG, that an adenosine CMR examination predicted with high sensitivity and specificity which patients had significant CAD during 1-year follow-up (60). Furthermore, Jahnke et al reported that a normal perfusion scan in patients with suspected CAD was predictive of a 99% chance of a 3-year event-free survival (36).

Each stress perfusion CMR is usually supplemented by late gadolinium enhancement (LGE) imaging, which delineates even small or subendocardial infarcted myocardium with high accuracy and robustness (9,61,62). Klem et al showed that a combined perfusion and infarction CMR examination is superior to stress perfusion CMR alone in the diagnosis of CAD (63). Furthermore, both a perfusion defect and the presence of LGE were independently associated with a more than three-fold increase in risk for cardiac death/MI, underscoring the complementary value of LGE imaging and stress perfusion CMR. Finally, even in the absence of any stress-induced perfusion defect during CMR testing, the detection of LGE is associated with a 13-fold increase in the risk of cardiac death/MI for the patient (59).

ASSESSMENT OF MYOCARDIAL INFARCTION USING CMR

In addition to enabling stress tests to assess the presence of myocardial ischemia in patients with known or suspected CAD, CMR also offers ways to detect and characterize MI—both in the acute and in the chronic state. Technological advances in CMR in the past have shortened acquisition times while improving image quality, enabling CMR exams to be performed even in patients with symptoms suspicious of acute MI and in the early phase following an acute event (64). There are two main CMR techniques that highlight the strength of CMR to assess MI. First, LGE imaging depicts irreversibly damaged myocardium that is present both acutely as necrosis, and chronically as fibrosis. It enables identification, verification and quantification of infarcted and scarred tissue, which can be used for the prediction of recovery of cardiac function after interventions or of patient outcome. Therefore, the speed and robustness of this technique is a great advantage that has promoted its widespread clinical application and acceptance (9). Second, T2-weighted imaging allows the detection of myocardial edema, which is present in the acute stage of myocardial injury and represents the area that is compromised from ischemia. Even though this CMR technique still suffers from imperfect robustness, it has immense potential as it is currently the only noninvasive modality that allows the assessment of myocardial edema (65).

Detection and Sizing of Infarcted Myocardium Using LGE Imaging

First attempts to visualize myocardial infarction by contrast enhanced CMR date back to the 1980s (66,67). In the mid and late 1990s, techniques using contrast-enhanced CMR for infarction detection were significantly improved (68,69), leading to image acquisitions specifically designed to achieve maximum contrast between infarcted and noninfarcted myocardium (70). The technique involves T1-weighted inversion-recovery imaging approximately 10 min after intravenous administration of gadolinium contrast. With appropriate settings, normal myocardium appears black or nulled, whereas nonviable regions appear bright or hyperenhanced. This pulse sequence increases regional differences in myocardial image intensities from approximately 50% to more than 500%, thereby significantly improving the visualization of hyperenhanced regions (Fig. 3). Phase-sensitive inversion recovery acquisitions can also be used, which are less dependent on the correct inversion time and thus may offer a more robust approach particularly for less experienced centers (71). Images are usually acquired during repeated breath holds both in long axis orientation and in a stack of short axis slices covering the left ventricle, to enable reporting in concordance with the AHA 17-segment model (17). Currently, navigator-based 3D image acquisitions (71), as well as free-breathing techniques are under investigation for clinical use (72,73).

The mechanism of LGE relies upon two assumptions: (a) The tissue volume in normal myocardium is predominately intracellular, because myocytes are densely packed; (b) Gadolinium chelates are extracellular agents that cannot cross intact sarcolemmal membranes. Therefore, the gadolinium distribution volume is small and tissue concentration is low in normal myocardium, whereas cell membrane rupture in acute necrosis allows gadolinium to diffuse into myocytes leading to increased gadolinium concentration, shortened T1 relaxation, and thus hyperenhancement. In the chronic setting, scar tissue replaces necrotic tissue and the interstitial space is expanded, which again results in increased gadolinium concentration and hyperenhancement (9).

Animal models demonstrated that LGE agrees very closely with histopathology regarding the size and shape of infarcted myocardium (61). In a landmark study, Wagner et al compared LGE imaging, SPECT and histopathology in 12 dogs with MI and found that even very small infarcts, as well as exclusively subendocardial infarctions, were detected by LGE with a sensitivity comparable to histopathology and clearly superior compared with nuclear medicine (61,74). Klein et al demonstrated that LGE is superior in detecting scar compared with wall thickness and wall thickening compared with positron emission tomography (PET) as the gold standard (75).

The detection of injury by LGE is specific for irreversible myocardial damage, but is not specific for MI. However, its pattern differs between ischemic and nonischemic heart disease. Therefore, it provides

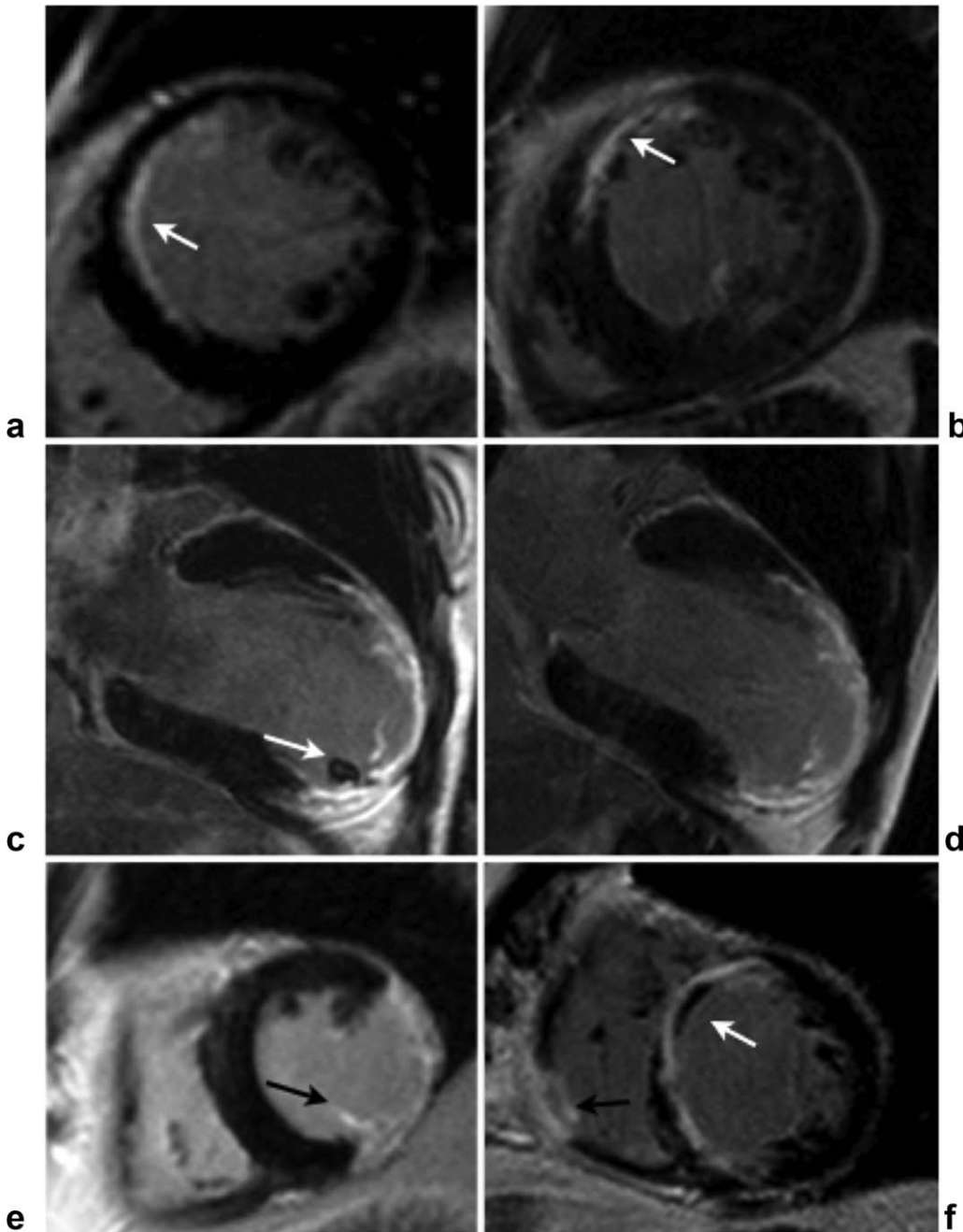


Figure 3. Various examples of LGE imaging in chronic ischemic heart disease. **a:** Subendocardial LGE of the anteroseptal wall (white arrow). **b:** Almost transmural LGE of the anteroseptal wall (white arrow). **c:** Thinned and scarred left ventricular apex with small thrombus (white arrow). **d:** Same patient as c) after 2 months with oral anticoagulation treatment. The thrombus disappeared completely. **e:** Infarction of the posterior papillary muscle (black arrow). **f:** Infarction of the right ventricular free wall (black arrow) and the septal wall with an adjacent thrombus (white arrow).

important information regarding the etiology of myocardial damage, which is crucial for the clinician. According to the wavefront phenomenon (76), ischemic lesions mostly affect the subendocardial layer, while the extension to the subepicardial portion is variable, and usually their distribution corresponds to the coronary territories. In contrast, nonischemic lesions—such as in inflammatory heart disease or cardiomyopathies—are predominantly located in the subepicardial or middle portion of the myocardium

with a more patchy distribution that is independent of the coronary territories (Fig. 4) (77,78).

Making the diagnosis of MI is not always straightforward in clinical cardiology. Blood markers of myocardial injury are elevated for only a few days after an acute event. Q waves on the ECG are quite unspecific. Wall motion abnormalities on TTE may not occur unless the infarcted region exceeds 20–50% of the myocardial wall; and SPECT defects may not be apparent until >10 g of tissue is infarcted (79). Conversely,

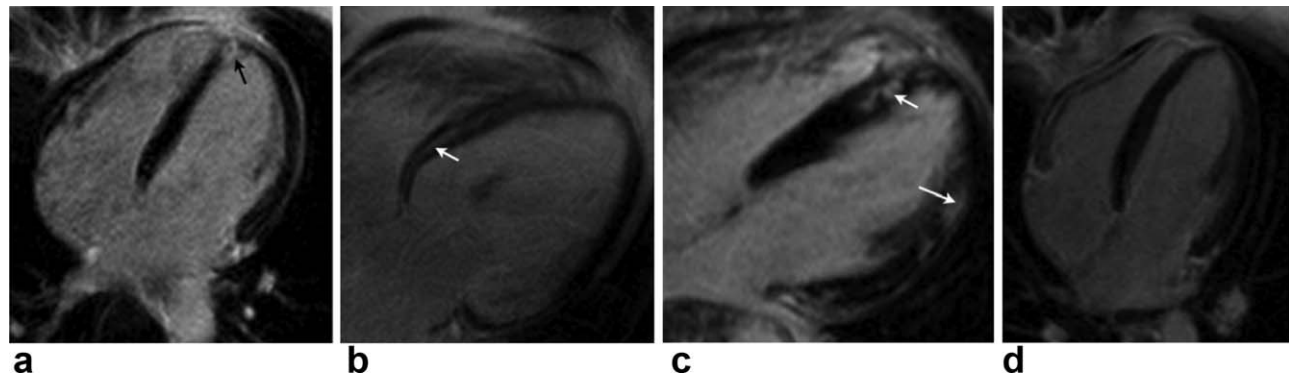


Figure 4. Determination of the type of myocardial injury by LGE imaging. Various examples depicted as a four-chamber view. **a:** Acute MI with small apical LGE with central microvascular obstruction (black arrows) in a patient with symptoms of MI but normal coronary angiography. **b:** Midwall LGE in the septal wall indicating dilated cardiomyopathy (white arrow). **c:** Patchy subepicardial and intramural LGE indicating inflammatory heart disease (white arrow). **d:** No LGE in a patient with Takotsubo cardiomyopathy.

nonischemic conditions, such as cardiomyopathies or inflammatory heart disease, can also lead to wall motion abnormalities, loss of viable myocardium, or elevated blood markers (77). As such, in situations where the diagnosis of MI is difficult, CMR is regarded to be very helpful. LGE imaging detects the presence of MI lesions with higher accuracy than any other noninvasive diagnostic modality. Wagner et al studied 91 patients with known or suspected CAD by CMR and SPECT. They found that all segments with nearly transmural infarction, as defined by contrast-enhanced CMR, were detected by SPECT as well. However, of the 181 segments with subendocardial infarction, 85 were not detected by SPECT. On a per patient basis, 13% of the individuals with subendocardial infarcts visible by CMR would have been missed by SPECT (61). Furthermore, an international multi-center trial confirmed a low observer dependency for MI detection by LGE imaging (62). Kwong et al reported that the prevalence of unrecognized MI by LGE was 76% higher than by ECG, which has enormous implications for patient management, e.g., starting medication for secondary prophylaxis (80). Even micro-infarctions, such as may occur during percutaneous coronary angioplasty, are detectable by CMR (81). LGE detects right ventricular involvement in MI more often than standard measures, which is important as right ventricular dysfunction following MI is associated with a worse prognosis (82,83) (Fig. 3f). LGE identifies infarction of the papillary muscle more frequently than previously thought and thus may impact considerations of valvular surgery—although it is controversial at present whether papillary muscle infarction affects mitral regurgitation and left ventricular remodeling (Fig. 3e) (84,85). Furthermore, although the best way to quantify infarct size by LGE is still under debate, this approach may provide a useful surrogate end point for clinical trials comparing various infarction therapies, and can lead to an appreciable reduction in required sample sizes (86).

Recent reports also indicate that CMR is able to detect fat deposition after MI. From a technical perspective, this can be achieved by T1-weighted images with/without

out fat suppression, or by using a three-point Dixon reconstruction from in- and opposed-phase black-blood gradient-echo images (87). Applying the latter method, Goldfarb et al found a fat deposition prevalence of 68% in areas of chronic MI. The extent of fat deposition was negatively associated with infarct size, wall motion, ejection fraction and left ventricular volume (88). Whether the presence of intramyocardial fat forms a substrate for arrhythmias or sudden cardiac death remains to be investigated. From a practical perspective, this approach is already useful in differentiating true LGE lesions from signal enhancement that may arise due to the presence of fat.

Detection of Acute Myocardial Infarction Using T2-Weighted Imaging

The documentation or exclusion of acute CAD is one of the most frequent and important tasks in clinical cardiology. Due to the need for fast decision making that mostly includes active and invasive interventions, CMR is usually not integrated into the workflow. However, several clinical constellations exist where the diagnosis remains unclear. Recently, evidence is accumulating that CMR can provide unique information in chest pain syndromes that can aid in the detection and differential diagnosis of acute MI, guide clinical decision making, and improve risk stratification after an event (89,90). In addition to LGE imaging, which delineates irreversibly injured myocardium, T2-weighted imaging has gained importance in this setting to improve tissue characterization (91,92).

Myocardial edema, increased myocardial water content, is a feature of many forms of acute myocardial injury that are associated with inflammation, such as ischemia or myocarditis. T2-weighted CMR imaging is sensitive to regional or global increases in myocardial water (65). The first report demonstrating the linear correlation between T2 relaxation time assessed by CMR and myocardial water content came from Higgins et al. who examined acutely infarcted myocardium (93). Using a spin echo acquisition, T2-weighted image contrast is achieved by imaging with a long

repetition time compared with tissue T1 (to reduce the T1 contribution to image contrast) and a long echo time in the range of the value of T2 in the tissue of interest. Tissues with longer T2 will have a higher signal in a T2-weighted acquisition. With the echo time set to 60–64 ms (typically used in clinical T2-weighted CMR imaging), free water becomes the most significant contributor to the T2 signal intensity in muscle tissue. In practice, myocardial segments with myocardial edema appear bright (Fig. 5e,f).

Recent advances in T2-weighted CMR could address many previous problems with low signal-to-noise ratio, coil-related signal-inhomogeneities and inconsistent image quality. Mostly, a breath-hold, black-blood, triple-inversion recovery turbo spin echo sequence is applied, although attempts using SSFP acquisitions have been performed (94,95). Similar to LGE, the pattern of distribution of bright zones on T2-weighted images may help to indicate the etiology of myocardial injury. In general, tissue alterations caused by ischemia lead to increased signal intensity in the subendocardium or—which is more common—transmurally in segments corresponding to the supplying coronary artery territories. In contrast, myocardial edema provoked by inflammatory/nonischemic heart disease tends to be located in the midventricular or subepicardial portion of the myocardium and appears independent from any supplying coronary artery territories (77,96).

Abdel-Aty et al recently showed in an animal model with temporary coronary artery occlusion that T2-weighted imaging of edema detects acute ischemic myocyte injury at a very early stage, even before the onset of irreversible damage occurs (97). These data support the potential use of this technique to evaluate cases of possible acute coronary syndrome using CMR. Furthermore, CMR offers a complementary approach that integrates T2-weighted imaging showing reversible myocardial injury—the so called “area-at-risk”—and LGE imaging showing irreversible myocardial damage. Up to now, the assessment of that area at risk required the injection of a radioactive tracer into the occluded coronary artery before revascularization. Instead, CMR provides a more attractive option, because it enables a retrospective determination of the area at risk, as both T2 and LGE characteristics are detectable even days after the acute event (89,98).

The combination of both sequences enables quantification of the extent of the salvaged area after revascularization, which is represented by the difference from the area at risk and LGE, and is an important parameter for clinical decision making and research (99). Francone et al demonstrated that in patients with ST-elevation MI treated with primary percutaneous coronary intervention, the time to reperfusion determines the extent of reversible and irreversible myocardial injury. In particular, salvaged myocardium was markedly reduced when reperfusion occurred >90 min after coronary occlusion (100). Furthermore, the combination of T2-weighted imaging with LGE imaging has been proven to be helpful in differentiating acute from chronic MI: While chronic MI is represented by LGE alone, acute MI is characterized both by high signal intensity in T2-weighted images and by LGE in the infarcted region (101). This is reported to be useful in the setting of delayed presenta-

tions after acute MI, in which cardiac markers may have returned to normal, whereas abnormalities on T2-weighted CMR can persist for several weeks (98,102). Another application of the combined approach is the management of patients presenting to the emergency department with acute chest pain, negative cardiac biomarkers, and no ECG changes indicative of acute ischemia. Cury et al found that T2-weighted imaging in addition to LGE and cine imaging led to an increase in specificity, positive predictive value and overall accuracy from 84% to 96%, 55% to 85%, and 84% to 93%, for the detection of acute MI. Therefore, CMR provided incremental value above traditional risk stratification, with the changes detected by CMR occurring before the rise in cardiac blood markers (64).

Assessment of Infarct Related Complications

Ventricular thrombus is a frequent complication of ischemic heart disease and increases the risk of stroke. In clinical cardiology, the diagnosis is usually made by echocardiography, even though the detection of ventricular thrombus is limited, in particular if thin thrombus coats the ventricular endocardium or if thrombus is located in the apex. CMR facilitates the detection of ventricular thrombus both by SSFP cine imaging with excellent blood-tissue contrast, as well as with the use of LGE imaging. The basic underlying principle for thrombus detection with LGE is that thrombi are avascular, and have essentially no gadolinium uptake. Thus, thrombus can be identified as a nonenhancing defect surrounded by bright ventricular blood and contrast-enhanced myocardium (Figs. 3c,f, 6b,c) (103). In patients with ischemic cardiac disease, LGE identified left ventricular thrombus in substantially more patients than cine CMR or TTE (104). Sri-chai et al compared LGE, TTE, and transesophageal echocardiography to detect left ventricular thrombus in patients who underwent surgical left ventricular aneurysmectomy. In this study LGE exhibited a higher sensitivity and specificity (88%/99%) compared with TTE (23%/96%) and transesophageal echocardiography (40%/96%) (105). In addition, CMR is a valuable tool to monitor the course of a ventricular thrombus during anticoagulation therapy due to the high reproducibility of slice positioning (Fig. 3c,d). However, it should be noted that the reported high diagnostic performance of CMR to identify thrombus only holds true for the ventricles, and not for the left atrium or left atrial appendage, because in this regard CMR is still limited by inadequate spatial and temporal resolution and the non-real-time acquisition. Thus, this indication would still require standard monitoring by means of transesophageal echocardiography.

The detection of postinfarction ventricular wall perforation is also facilitated by CMR due to its three-dimensional approach, such that even complex morphological changes can be detected. (Fig. 6a–c). Finally, CMR including LGE imaging can help to attribute unusual ventricular morphology as detected by other imaging modalities to postinfarction remodeling (Fig. 6d–f), which has a significant impact on patient management.

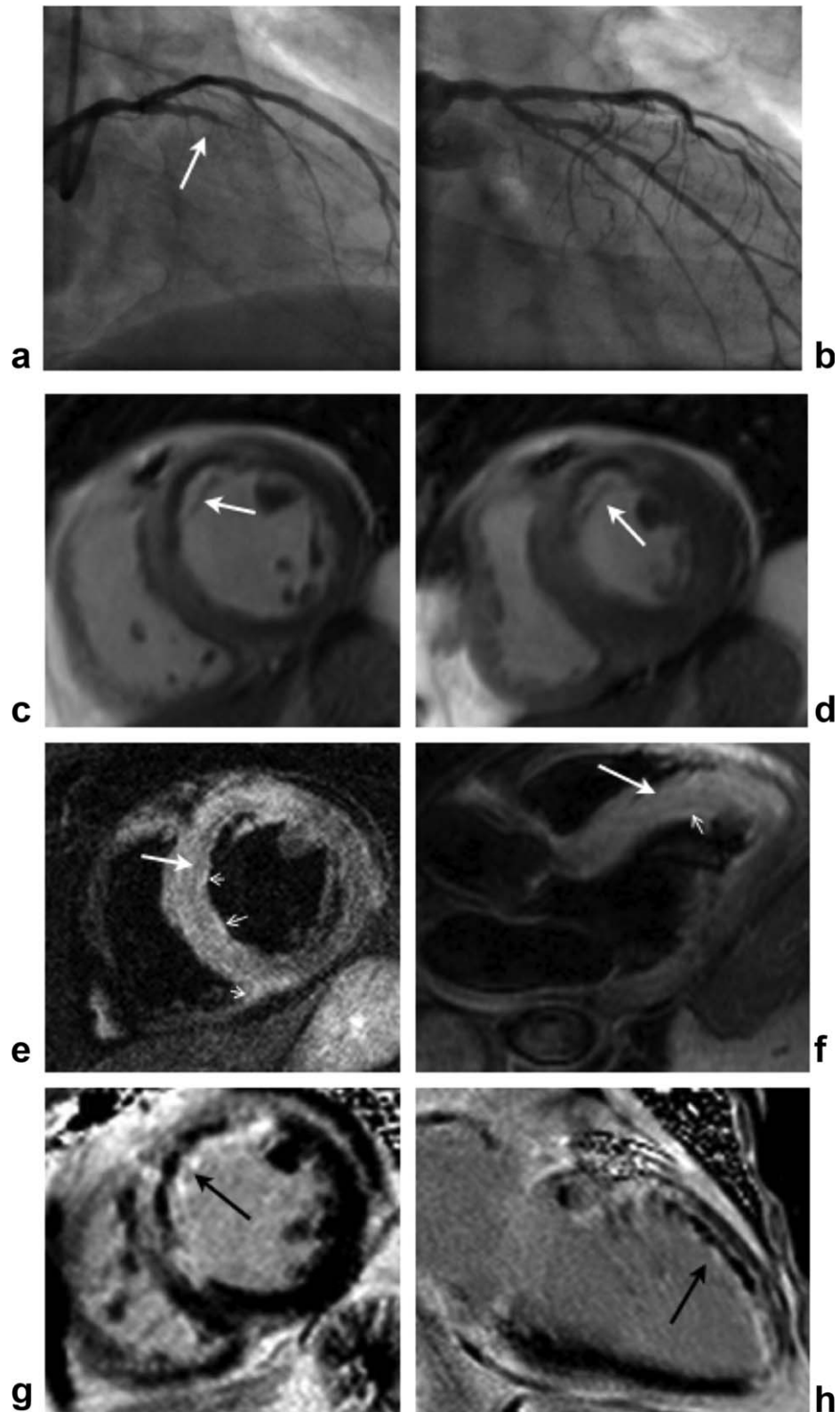


Figure 5. Multiparametric CMR imaging in a 69-year-old patient, who was admitted to hospital with acute MI the day before. **a,b:** Coronary angiography revealed occlusion of the left anterior descending artery, which was reopened and treated with stent implantation (white arrows). **c,d:** SSFP cine imaging in diastole and systole (after contrast media administration) showed anteroseptal akinesia and microvascular obstruction (white arrows). **e,f:** T2-weighted imaging demonstrated myocardial edema and thickening of the anteroseptal wall (white arrows). Small areas with high signal intensity caused by slow blood flow are highlighted by open arrow heads. **g,h:** LGE imaging delineated extensive myocardial infarction of the anteroseptal wall, extending the myocardial edema, and including a dark core with microvascular obstruction (white arrows).

Assessment of Myocardial Viability

From a clinical perspective, myocardial viability suggests that the systolic function of an infarcted region will recover after revascularization. Thus, viability testing should predict the myocardial response to revascularization. There are several approaches to

assess myocardial viability by CMR, although LGE imaging is the predominant method:

Myocardial Wall Thickness

As chronic scar formation is associated with thinned myocardium, cut-offs for end diastolic myocardial

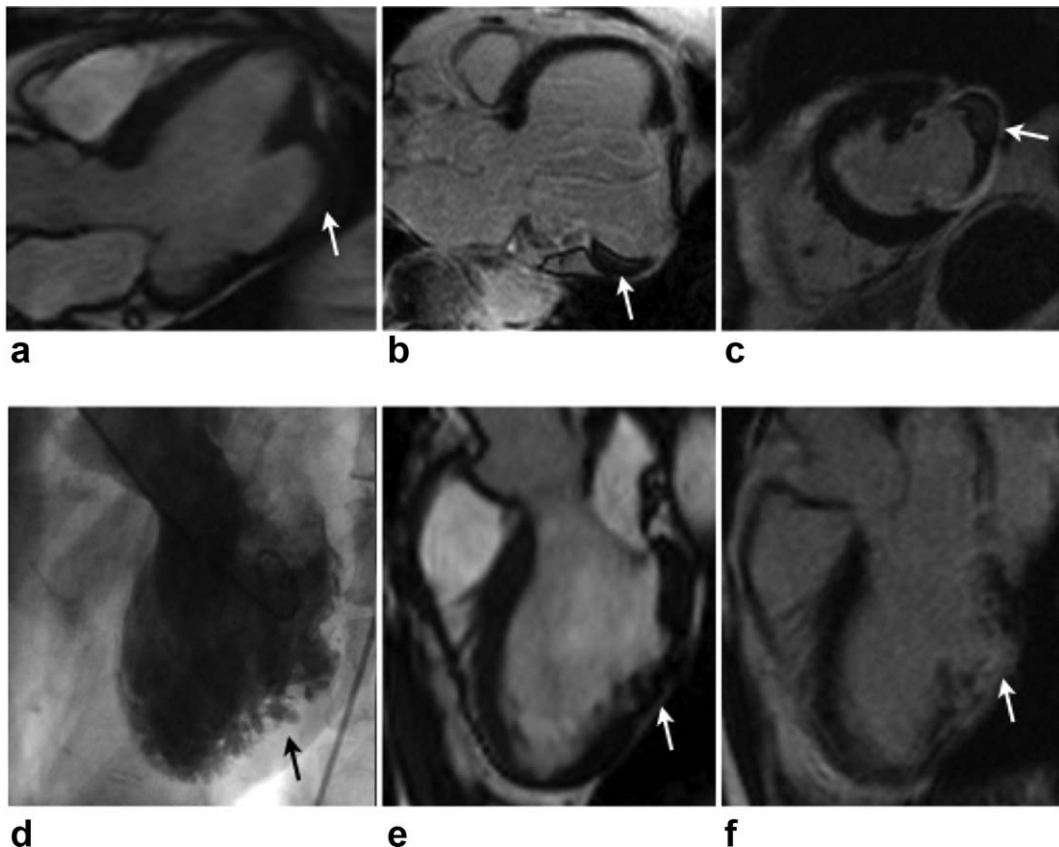


Figure 6. Postinfarction complications: Upper panel: A 66-year-old woman who suffered from one episode of severe chest pain. Coronary angiography was reported to be normal. Thus, the patient was referred to undergo CMR to rule out myocarditis. **a:** Three-chamber view with SSFP acquisition demonstrating an abnormal inferolateral wall (white arrow). **b,c:** Three-chamber and short axis view with LGE technique showing inferolateral wall rupture with thrombus (white arrow), providing evidence of previous MI. Lower panel: A 50-year-old woman needed resuscitation due to ventricular arrhythmia. **d:** Cardiac catheterization ruled out coronary artery stenosis, but reported hypertrabecularization of the inferolateral wall (black arrow) suggested a form of cardiomyopathy as the underlying cause of sudden cardiac death. **e:** CMR with SSFP acquisition confirmed abnormal inferolateral wall morphology (white arrow). **f:** LGE imaging demonstrated transmural infarction-type scar as the underlying cause (white arrow). Thus, the patient was treated as postinfarction patient instead of having another type of cardiomyopathy.

wall thickness as assessed by CMR cine imaging were proposed to assess myocardial viability. Whereas, for instance, the negative predictive accuracy of a cut-off of 5.5 mm was satisfactory with 90%, its positive predictive accuracy was only 62% (106). This unfavorable diagnostic performance is explained by the fact that simply looking at wall thickness by CMR does not consider its morphology. Hence, this approach does not discriminate between viable and nonviable proportions of the ventricular wall. Furthermore, this approach does not define the thickness of the remaining viable rim, which is the most important factor in determining whether a segment will recover function.

Low-Dose Dobutamine

As with low-dose dobutamine TTE, low-dose dobutamine CMR has been introduced to assess myocardial viability. In this case, repeated cardiac cine images are acquired at rest and at 5 and 10 $\mu\text{g}/\text{kg}/\text{min}$ dobutamine infusion to assess left ventricular contractile reserve. Despite achieving satisfactory diagnostic accuracy—Baer et al reported a sensitivity in predicting recovery of left ventricular function after revasculariza-

tion of 89% and a specificity of 94% on a patient-basis (107)—this approach was widely replaced by LGE imaging (see next point) due to its speed and robustness as well as its higher accuracy, especially in more severe cardiac dysfunction. Nevertheless, it is recommended to add low-dose dobutamine CMR to LGE imaging in those LGE studies that remain inconclusive (see next point) (7,108). Furthermore, low-dose dobutamine is an adequate approach in patients with contraindications to Gadolinium.

LGE Imaging

LGE imaging has been demonstrated to be superior to detect myocardial scarring compared with wall thickness and wall thickening on cine imaging (75). Therefore, LGE imaging is generally regarded as a better predictor for myocardial recovery compared with the assessment of wall thickness and thickening alone. Furthermore, LGE imaging does not only evaluate the mere presence or absence of myocardial scarring, but also allows the determination of the transmural extent of a myocardial lesion within a segment (Fig. 3a,b) (75). In a landmark study, Kim et al

assessed the transmurality of LGE 41 patients with ventricular dysfunction before and approximately 3 months after surgical or percutaneous revascularization. In an analysis of all 804 dysfunctional segments, the likelihood of improvement in regional contractility after revascularization decreased progressively as the transmural extent of hyperenhancement before revascularization increased. For instance, contractility increased in 256 of 329 segments (78%) with no hyperenhancement before revascularization, but in only 1 of 58 segments with hyperenhancement of more than 75 percent of tissue. The percentage of the left ventricle that was both dysfunctional and not hyperenhanced before revascularization was strongly related to the degree of improvement in the global mean wall-motion score and the ejection fraction after revascularization (109). Similar results were reported by Selvanayagam et al, who studied 52 patients before and 6 months after coronary bypass surgery (110). Preoperatively, 611 segments (21%) had abnormal regional function, whereas 421 segments (14%) showed evidence of hyperenhancement. At 6 months after revascularization, 57% (343 of 611) of dysfunctional segments improved contraction by at least one grade. When all preoperative dysfunctional segments were analyzed, there was a strong correlation between the transmural extent of hyperenhancement and the recovery in regional function at 6 months.

However, both studies also identified a grey zone, where functional improvement following revascularization was uncertain, if scar transmurality was between 1 and 50%. In these cases, the additional performance of a CMR study with low-dose dobutamine to assess inotropic contractility of the myocardial wall has been shown to improve clinical accuracy (7,108,111). Glaveckaite et al recently reported that low dose dobutamine is even superior to LGE imaging as a predictor of segmental recovery when applied specifically to segments with an LGE from 26% to 75%. Similarly, Kirschbaum et al reported that quantification of the extent of segmental wall thickening of the viable rim during low dose dobutamine is a superior predictor of functional recovery than LGE transmurality (112).

In addition, the extent of nonenhanced myocardium contributes to the recovery of myocardial function. Ichikawa et al reported that measurement of thickness of nonenhanced myocardium, compared with measurement of percent transmural enhancement, had even better diagnostic accuracy for predicting improved systolic wall thickening in dysfunctional segments in 18 patients following acute MI. They showed that the optimal threshold of the thickness of nonenhanced myocardium for predicting preserved systolic wall thickening in the chronic state was 3.9 mm (113). Similarly Glaveckaite reported a cut-off of 4 mm that produced the best sensitivities and specificities for predicting segmental recovery in 46 patients 6 months following revascularization (114).

Risk Stratification in Ischemic Heart Disease

CMR provides several parameters that offer an estimate of cardiac remodeling and prognosis on the individual patient level following an acute MI. This information is of eminent clinical relevance to determine the optimal therapeutic pathway for each subject to omit over- and under-treatment.

The mere presence of scar resulting from MI conferred nearly a six-fold increased risk for major cardiac events—even if only approximately 1% of the left ventricle was affected (80,115). Infarct size is a stronger predictor of outcome than left ventricular ejection fraction and volumes (116). Kwon et al found that in patients with ischemic cardiomyopathy and severely reduced ejection fraction, a greater extent of myocardial scar, delineated by LGE, was associated with increased mortality (117). Boye et al recently reported that in particular the degree of infarct transmurality identified a subgroup with increased risk for life-threatening arrhythmias and cardiac death in patients with chronic MI (118). In addition, the composition of LGE, likely representing the admixture of viable and nonviable myocardium within an infarcted region, may influence the prognosis and the incidence of ventricular arrhythmia (119). Thus, in the future LGE imaging may improve risk stratification following MI, and help to identify those subjects who would benefit most from prophylactic implantation of an internal cardioverter defibrillator. This therapy is currently mainly determined by the severity of reduction in systolic function, but a significant percentage of implantations occur in patients in whom the device is never called upon (120). However, in order for LGE to be fully incorporated as a criterion of risk stratification, a robust technique to accurately define the extent of scar and grey area is needed (121).

Etel et al showed that the so-called myocardial salvage index (calculated as the area at risk (assessed by T2-weighted imaging) minus the infarct size (assessed by LGE imaging) divided by the area at risk) predicts the outcome in acute reperfused ST-elevation MI. They found a significantly lower mortality and major adverse cardiovascular events rate after 6 months for the group with a smaller myocardial salvage index than the median of the sample (122). T2-weighted imaging seems to add prognostic information even in patients with non-ST-elevation MI. In a study by Raman et al, patients with edema showed a higher risk of a cardiovascular event or death within 6 months compared with those without edema (123). Furthermore, CMR has been proposed for the assessment of myocardial hemorrhage, which appears as a hypointense core within the hyperintense edema on T2-weighted imaging (Fig. 7a). In a study by Ganame et al, myocardial hemorrhage was an independent predictor of adverse left ventricular remodeling at four months follow-up, independent of the initial infarct size (124). Similarly, Mather et al reported that reperfusion hemorrhage following acute MI was associated with larger infarct size, diminished myocardial salvage, lower left ventricular ejection fraction, adverse ventricular remodeling and pronounced ECG features indicating higher arrhythmic risk (125).

Another prognostic parameter that can be determined by CMR is the proof of microvascular obstruction (MVO), or no-reflow despite reperfusion of the

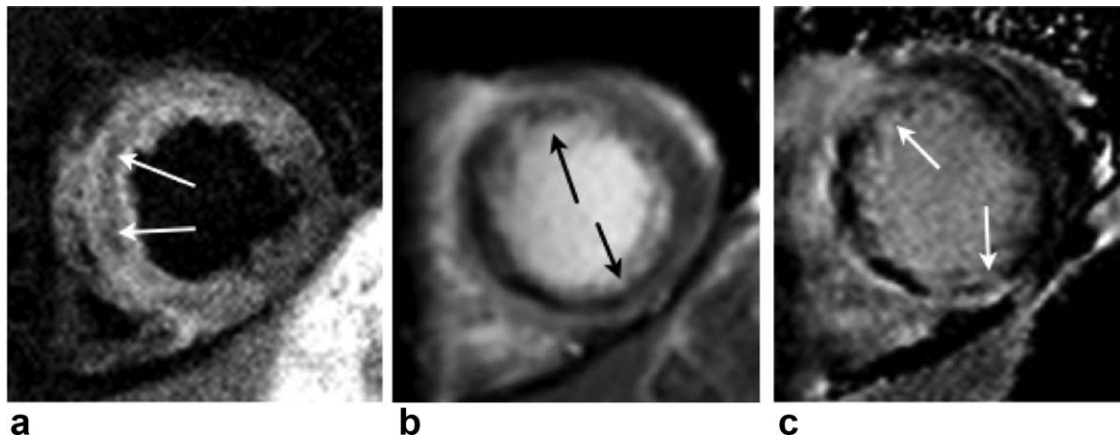


Figure 7. CMR examination of a 59-year-old man, who presented with acute ST-elevation MI due to early stent thrombosis in the left anterior descending artery and underwent revascularization. **a:** T2-weighted imaging reveals a large area of edema including a dark central region thought to represent hemorrhage (white arrows). **b:** SSFP cine imaging early after contrast media administration depicts the large extent of microvascular obstruction, visible as a dark band (white arrows). **c:** LGE imaging delineates the size of MI with microvascular obstruction (white arrows).

epicardial coronary arteries. MVO can be summarized as reperfusion injury and is the consequence of clogging of small myocardial arterioles with embolic debris, acute inflammation, platelet aggregation and vasospasm (126). The presence of MVO is a marker for unfavorable cardiac remodeling and prognosis. Assessed by CMR, MVO either appears as a hypointense area during first-pass perfusion at rest, as a hypointense core during early gadolinium enhancement imaging at 1 to 2 min after contrast agent injection, or as a hypointense core within the bright region of an infarction during LGE imaging (Figs. 4a, 5c,d,g,h, 7b, c). It is still a continuing debate which technique is the best to assess MVO by CMR. Perfusion imaging was found to be more sensitive for the detection of MVO compared with LGE, however is hampered by incomplete left ventricular coverage, low signal-to-noise ratio, and low spatial resolution. Experimental studies have demonstrated that the spatial extent as well as location of early MVO closely correlate with histopathological analyses. LGE-CMR underestimates the extent of MVO as compared to perfusion imaging and might miss small regions of MVO due to slow penetration of contrast into the MVO region over time. On the other hand, late MVO seems to be a more important prognostic indicator compared with early MVO. Hence, ideally the imaging protocols should combine perfusion imaging, early imaging and LGE to overcome the limitations of each method (126). Anyway, the fact remains that CMR-driven detection of MVO has an additional prognostic impact beyond the use of left ventricular ejection fraction. Hence, the use of MVO itself should be explored in the clinical arena. De Waha et al reported that the presence and extent of late MVO were independently associated with a composite end-point comprising death, nonfatal myocardial re-infarction and congestive heart failure (127). Nijveldt et al demonstrated in patients after revascularized acute MI that the presence or absence of MVO proved a more powerful pre-

dictor of global and regional functional recovery than other characteristics such as TIMI flow grade, myocardial blush grade, ST-segment resolution and even infarct size and transmural extent as assessed by CMR (128). Similarly, Hombach et al found microvascular obstruction to be a highly sensitive and reliable tool to detect morphologic and functional sequelae of acute MI that predict adverse cardiac remodeling and the occurrence of major adverse cardiovascular events (129).

Discrimination of Differential Diagnosis of Acute Ischemic Heart Disease

As mentioned previously, both LGE and T2-weighted imaging provide pathologic patterns that can indicate the etiology—ischemic versus nonischemic—of an acute event or an active inflammatory reaction, respectively. This capability has strong clinical relevance, as a nontrivial proportion of up to 10% of patients initially diagnosed with ST-elevation MI, and 32% of patients presenting with acute coronary syndrome, turn out to have normal coronary arteries at invasive coronary angiography (9). CMR helps to find the correct diagnosis, which may be Takotsubo cardiomyopathy with reversible wall motion abnormalities, edema extending over one coronary artery territory, and the absence of LGE; or myocarditis with subepicardial and intramural LGE lesions and global or patchy edema; or myocardial infarction despite normal coronary arteries, with subendocardial LGE and edema fitting to MI, possibly indicating spontaneous intracoronary thrombolysis (Fig. 4) (77). In a registry of 1335 MI patients undergoing coronary angiography, Larson et al reported that 14% had no culprit artery and 9.5% did not have significant CAD. In the group without a clear culprit artery, CMR established that the most common diagnoses were myocarditis (31%), Takotsubo cardiomyopathy (31%), and MI without an angiographic lesion (29%) (130).

CHALLENGES OF CMR IN ISCHEMIC HEART DISEASE

Despite the enormous technological progress of CMR and the numerous clinical data that support its application, there are still many challenges to be solved to increase the robustness and accuracy of this method and to promote its widespread use. In the following text, some examples regarding the use of CMR in ischemic heart disease are discussed:

Dobutamine Stress CMR

With the occurrence of any new wall motion abnormality during dobutamine infusion, the adverse event rate of this stress test increases. Therefore, real-time detection of the onset of cardiac dysfunction and immediate discontinuation of the dobutamine infusion is warranted to increase patients' safety. Hence, the implementation of high resolution real-time CMR imaging during dobutamine stress would be desirable.

Perfusion stress CMR

Using the most frequently applied approach, three short axes that are planned at rest and imaged during stress perfusion are currently the best available LV coverage in clinical routine. However, the faster cardiac movement due to stress-induced tachycardia and the dyspnea-related altered breath hold position sometimes lead to a shift of the three short axes, so that the left ventricular myocardium is not represented completely any more. In addition, respiratory motion, which occurs at least once during first-pass perfusion acquisition, and ECG trigger problems during deep respiratory motion further promote constraints of the image quality. Finally, the presence of dark rim artifacts is still a relevant clinical problem, particularly in centers with less experience. Thus, many technical solutions are needed to implement stress perfusion CMR as a routine stress test in clinical cardiology, e.g., three-dimensional approaches with high spatial resolution and local registration to allow for free breathing.

LGE Imaging

Although LGE imaging is a robust technique, the delineation of thin subendocardial LGE from the bright contrast enhanced blood pool is sometimes difficult. Therefore, techniques that facilitate this differentiation are needed. Furthermore, patients with ischemic heart disease and heart failure often struggle with the repeated breath holdings during LGE imaging, particularly if it is performed in the end of a long lasting examination. Robust sequences, which allow free breathing, but still provide the resolution of standard acquisitions, are needed. Finally, the quantification of LGE is still under debate. Currently, the preferred method for LGE quantification is to planimeter the infarct visually using experienced readers, who can carefully segment myocardial borders and

account for artifacts and areas with intermediate image intensity. In contrast, semiautomatic methods, which use image thresholds of 2 to 7 standard deviations above the mean of remote normal myocardial intensity or a threshold value of 50% of the maximum intensity within the infarct (full width half maximum), are not as objective as one might think. Most require user input to distinguish artifacts, to trace the myocardial borders, and to define remote myocardium, leading to significant observer dependency (9,131). Furthermore, the latency between contrast media administration and image acquisition, and the type of contrast media, influence the extent of LGE (132). Thus, both international standards and technical improvements to allow for automatic LGE quantification are needed to promote a quantitative approach when assessing LGE images. At present, routine assessments are conducted visually.

T2-weighted Imaging

Whereas the method gives significant insights into myocardial injury, challenges regarding robustness and resolution of T2-weighted imaging still have to be improved, and lead to a potential impairment of the image quality, e.g., with high heart rates and thin myocardium.. Furthermore, image acquisition times (and thus the duration of breath holding) is long, causing respiratory artifacts in many patients (133). Therefore, new techniques are needed to strengthen the role of T2-weighted imaging and to fully exploit its unique potential, as T2-weighted imaging is currently the only noninvasive method to assess the presence and extent of myocardial edema, and has, therefore, a significant clinical need and impact. Another approach is to directly measure the T2 relaxation time on a pixel basis by T2-mapping. Initial reports with this technique are promising, but further validation is required in future studies (134).

FUTURE PERSPECTIVES OF CMR IN ISCHEMIC HEART DISEASE

Many innovations over previous years have entered clinical routine, and many more ideas are looming on the (pre-)clinical horizon. However, when developing new methods and assessing new inventions, the proof of concept should always be their robust application in a clinical setting and their accuracy to detect diseases, including their potential to influence patients' outcome. It would be beyond the scope of the present article to cover all promising developments in the field of CMR to assess patients with CAD. Hence, just a small selection of these current developments is presented to illustrate this active field of research.

Blood oxygen level dependent (BOLD) imaging is based on the principle that decreased oxyhemoglobin and increased deoxyhemoglobin tissue content result in lower T2* or T2 values, that lead to corresponding signal enhancement on T2* or T2-weighted imaging (135,136). While at 1.5T this technique suffered from low signal-to-noise ratio, this technique might

benefit from higher field strength. Further technical developments may enhance this promising method in the future, and with BOLD an additional tissue marker—complementary to the T1 and T2-weighted images described above—may arise (137,138).

Coronary angiography by CMR to visualize coronary artery stenosis is still inferior to computed tomography regarding its quantitative clinical usage, predominantly due to its methodological complexity and constraints of temporal and spatial resolution. High temporal resolution is needed to obtain motion-free images of the coronary arteries, which show rapid movement during the cardiac cycle. In addition, high spatial resolution is required to adequately visualize small coronary artery segments, ranging in diameter from a few millimeters proximally to submillimeter size more distally. Nevertheless, recent studies applying new technologies and higher main magnetic field strength have shown promising results (139). Kato et al reported that noncontrast-enhanced whole-heart CMR coronary angiography at 1.5T can noninvasively detect significant CAD—as assessed by coronary angiography—with high sensitivity (88%), moderate specificity (72%) and a satisfactory negative predictive value of 88% in a multi-center study (140). A recent comparison between CMR coronary angiography using a 32 channel coil with a 3T scanner, and 64-slice computed tomography angiography, showed that both methods similarly identify significant coronary stenosis in patients with suspected or known CAD scheduled for coronary angiography (141).

However, the isolated detection of any coronary lumen loss neither provides information regarding the hemodynamic relevance—as outlined above in the CMR perfusion chapter—nor does it predict the site where a coronary event is imminent. Therefore, it seems to be more important to exploit the potential of CMR to characterize the morphology and function of the coronary wall—incorporating measures of plaque composition, vessel wall inflammation, endothelial function, distensibility, or blood flow (142). These topics are currently fields of very active research. For instance, Hays et al described a noninvasive approach to directly visualize endothelial-dependent coronary artery dilation and increased blood flow in healthy subjects, and their absence in CAD patients by combining phase contrast flow measurements at 3T with handgrip exercise (143). Ibrahim et al analyzed the coronary artery wall in patients following acute MI using contrast-enhanced CMR. They detected changes in the extent and intensity of coronary contrast enhancement with the potential to visualize inflammatory activity in atherosclerosis associated with acute coronary syndrome (144). Lin et al obtained MR coronary angiographies in healthy and diabetic humans and observed significant differences in the coronary distensibility index (145). Regarding molecular imaging, Makowski et al established an elastin-specific MR contrast agent to noninvasively quantify and characterize plaque burden in a mouse model of atherosclerosis (146). Despite these encouraging results, restrictions in spatial and temporal resolution still limit robust assessment of the coronary arteries, and

must be overcome to fully exploit the potential of CMR for coronary evaluation.

CMR at ultrahigh field strength is thought to enable higher spatial and temporal resolution and faster imaging techniques. These benefits promise to improve tissue characterization in ischemic heart disease by giving more detailed insight into the texture and function of infarcted myocardium and the surrounding tissue. One theoretical future application of this technique could involve the detection of preclinical microinfarcts as precursors of overt infarcts. However, increasing the field strength leads to enormous technological challenges. Therefore, CMR at 7T is at present only applied in preclinical studies. Initial reports have demonstrated that cine imaging can be realized in a robust and accurate mode at 7T, with visualization of the right coronary artery demonstrated (147,148). However, to date, there have been no studies exploring this technique in patients with ischemic heart disease, or with infarct imaging at 7T *in vivo*. Hence, further developments in hardware and software are required to evaluate the clinical impact of ultrahigh field CMR in ischemic heart disease. Nevertheless, recent *ex vivo* animal studies of infarcted hearts at 7T demonstrated detailed, nearly cellular, insights for detection of fibrosis after MI (121). Especially this area can only be improved and developed based on a close collaboration between physicists, engineers and clinicians.

Diffusion tensor CMR has been introduced as a method to resolve microstructural fiber anatomy of the heart. Associations between tissue integrity and both fiber architecture and ventricular function after MI have been reported (149). Hence, this method may be a valuable tool in the future to analyze interactions between myocardial tissue morphology and function. However, hardware limitations of most clinical scanners constitute a barrier to progress at present. Hence, modern gradient systems and advances in radiofrequency technology, multi-element arrays, navigators, and parallel acquisition schemes are required to promote clinical translation of this technique (150).

CONCLUSION

CMR has become an important diagnostic element during the clinical work-up of patients with known or suspected ischemic heart disease. Hence, ischemic heart disease has become the most frequent indication to perform a CMR study. CMR provides information about cardiac dimensions, function, and myocardial perfusion with high robustness and accuracy. Furthermore, CMR gives unique insights into myocardial tissue alterations during acute and chronic ischemic heart disease. This noninvasive and radiation-free combined approach of functional and morphologic cardiac assessment with CMR provides unique characteristics and strengths compared with other imaging modalities. CMR allows the early detection of ischemic heart disease, and differentiation of nonischemic disorders, improves patient monitoring during the course of disease, provides additional information

for risk stratification and guidance of patient therapy. However, further developments are required to promote the widespread use of CMR as a routine clinical tool, including improved technical robustness, facilitated work-flow of a routine CMR study, and improved CMR training of clinicians.

ACKNOWLEDGMENT

We thank Dr. Victoria Claydon for carefully editing the manuscript.

REFERENCES

- Roger VL, Go AS, Lloyd-Jones DM, et al. Heart disease and stroke statistics—2011 update: a report from the American Heart Association. *Circulation* 2011;123:e18–e209.
- Bonow RO. Clinical practice. Should coronary calcium screening be used in cardiovascular prevention strategies? *N Engl J Med* 2009;361:990–997.
- Hundley WG, Bluemke DA, Finn JP, et al. ACCF/ACR/AHA/NASCI/SCMR 2010 expert consensus document on cardiovascular magnetic resonance: a report of the American College of Cardiology Foundation Task Force on Expert Consensus Documents. *Circulation* 2010;121:2462–2508.
- Beek AM, van Rossum AC. Cardiovascular magnetic resonance imaging in patients with acute myocardial infarction. *Heart* 2010;96:237–243.
- Karamitsos TD, Dall'Armellina E, Choudhury RP, Neubauer S. Ischemic heart disease: comprehensive evaluation by cardiovascular magnetic resonance. *Am Heart J* 2011;162:16–30.
- Bruder O, Schneider S, Nothnagel D, et al. EuroCMR (European Cardiovascular Magnetic Resonance) registry: results of the German pilot phase. *J Am Coll Cardiol* 2009;54:1457–1466.
- Charoenpanichkit C, Hundley WG. The 20 year evolution of dobutamine stress cardiovascular magnetic resonance. *J Cardiovasc Magn Reson* 2010;12:59.
- Gerber BL, Raman SV, Nayak K, et al. Myocardial first-pass perfusion cardiovascular magnetic resonance: history, theory, and current state of the art. *J Cardiovasc Magn Reson* 2008;10:18.
- Kim HW, Farzaneh-Far A, Kim RJ. Cardiovascular magnetic resonance in patients with myocardial infarction: current and emerging applications. *J Am Coll Cardiol* 2009;55:1–16.
- Gibbons RJ, Balady GJ, Bricker JT, et al. ACC/AHA 2002 guideline update for exercise testing: summary article: a report of the American College of Cardiology/American Heart Association Task Force on Practice Guidelines (Committee to Update the 1997 Exercise Testing Guidelines). *Circulation* 2002;106:1883–1892.
- Gould KL. Does coronary flow trump coronary anatomy? *JACC Cardiovasc Imaging* 2009;2:1009–1023.
- Panting JR, Gatehouse PD, Yang GZ, et al. Abnormal subendocardial perfusion in cardiac syndrome X detected by cardiovascular magnetic resonance imaging. *N Engl J Med* 2002;346:1948–1953.
- Vogel-Claussen J, Skrok J, Dombroski D, et al. Comprehensive adenosine stress perfusion MRI defines the etiology of chest pain in the emergency room: comparison with nuclear stress test. *J Magn Reson Imaging* 2009;30:753–762.
- Petersen SE, Jerosch-Herold M, Hudsmith LE, et al. Evidence for microvascular dysfunction in hypertrophic cardiomyopathy: new insights from multiparametric magnetic resonance imaging. *Circulation* 2007;115:2418–2425.
- Pennell DJ, Underwood SR, Manzara CC, et al. Magnetic resonance imaging during dobutamine stress in coronary artery disease. *Am J Cardiol* 1992;70:34–40.
- Mandapaka S, Hundley WG. Dobutamine cardiovascular magnetic resonance: a review. *J Magn Reson Imaging* 2006;24:499–512.
- Cerdeira MD, Weissman NJ, Dilsizian V, et al. Standardized myocardial segmentation and nomenclature for tomographic imaging of the heart: a statement for healthcare professionals from the Cardiac Imaging Committee of the Council on Clinical Cardiology of the American Heart Association. *Circulation* 2002;105:539–542.
- Wahl A, Paetsch I, Gollesch A, et al. Safety and feasibility of high-dose dobutamine-atropine stress cardiovascular magnetic resonance for diagnosis of myocardial ischaemia: experience in 1000 consecutive cases. *Eur Heart J* 2004;25:1230–1236.
- Kuijpers D, Janssen CH, van Dijkman PR, Oudkerk M. Dobutamine stress MRI. Part I. Safety and feasibility of dobutamine cardiovascular magnetic resonance in patients suspected of myocardial ischemia. *Eur Radiol* 2004;14:1823–1828.
- Geleijnse ML, Krenning BJ, Nemes A, et al. Incidence, pathophysiology, and treatment of complications during dobutamine-atropine stress echocardiography. *Circulation* 2010;121:1756–1767.
- Nagel E, Lehmkohl HB, Bocksch W, et al. Noninvasive diagnosis of ischemia-induced wall motion abnormalities with the use of high-dose dobutamine stress MRI: comparison with dobutamine stress echocardiography. *Circulation* 1999;99:763–770.
- Hundley WG, Hamilton CA, Thomas MS, et al. Utility of fast cine magnetic resonance imaging and display for the detection of myocardial ischemia in patients not well suited for second harmonic stress echocardiography. *Circulation* 1999;100:1697–1702.
- Nandalur KR, Dwamena BA, Choudhri AF, Nandalur MR, Carlos RC. Diagnostic performance of stress cardiac magnetic resonance imaging in the detection of coronary artery disease: a meta-analysis. *J Am Coll Cardiol* 2007;50:1343–1353.
- Wahl A, Paetsch I, Roethemeyer S, Klein C, Fleck E, Nagel E. High-dose dobutamine-atropine stress cardiovascular MR imaging after coronary revascularization in patients with wall motion abnormalities at rest. *Radiology* 2004;233:210–216.
- Syed MA, Paterson DI, Ingkanisorn WP, et al. Reproducibility and inter-observer variability of dobutamine stress CMR in patients with severe coronary disease: implications for clinical research. *J Cardiovasc Magn Reson* 2005;7:763–768.
- Paetsch I, Jahnke C, Ferrari VA, et al. Determination of interobserver variability for identifying inducible left ventricular wall motion abnormalities during dobutamine stress magnetic resonance imaging. *Eur Heart J* 2006;27:1459–1464.
- Lubbers DD, Janssen CH, Kuijpers D, et al. The additional value of first pass myocardial perfusion imaging during peak dose of dobutamine stress cardiac MRI for the detection of myocardial ischemia. *Int J Cardiovasc Imaging* 2008;24:69–76.
- Gebker R, Jahnke C, Manka R, et al. Additional value of myocardial perfusion imaging during dobutamine stress magnetic resonance for the assessment of coronary artery disease. *Circ Cardiovasc Imaging* 2008;1:122–130.
- Gebker R, Mirelis JG, Jahnke C, et al. Influence of left ventricular hypertrophy and geometry on diagnostic accuracy of wall motion and perfusion magnetic resonance during dobutamine stress. *Circ Cardiovasc Imaging* 2010;3:507–514.
- Kuijpers D, Ho KY, van Dijkman PR, Vliegenthart R, Oudkerk M. Dobutamine cardiovascular magnetic resonance for the detection of myocardial ischemia with the use of myocardial tagging. *Circulation* 2003;107:1592–1597.
- Paetsch I, Foll D, Kaluza A, et al. Magnetic resonance stress tagging in ischemic heart disease. *Am J Physiol Heart Circ Physiol* 2005;288:H2708–H2714.
- Korosoglou G, Lossnitzer D, Schellberg D, et al. Strain-encoded cardiac MRI as an adjunct for dobutamine stress testing: incremental value to conventional wall motion analysis. *Circ Cardiovasc Imaging* 2009;2:132–140.
- Kelle S, Hamdan A, Schnackenburg B, et al. Dobutamine stress cardiovascular magnetic resonance at 3 Tesla. *J Cardiovasc Magn Reson* 2008;10:44.
- Hundley WG, Morgan TM, Neagle CM, Hamilton CA, Rerkpattanapipat P, Link KM. Magnetic resonance imaging determination of cardiac prognosis. *Circulation* 2002;106:2328–2333.
- Kuijpers D, van Dijkman PR, Janssen CH, Vliegenthart R, Zijlstra F, Oudkerk M. Dobutamine stress MRI. Part II. Risk stratification with dobutamine cardiovascular magnetic resonance in patients suspected of myocardial ischemia. *Eur Radiol* 2004;14:2046–2052.
- Jahnke C, Nagel E, Gebker R, et al. Prognostic value of cardiac magnetic resonance stress tests: adenosine stress perfusion and

- dobutamine stress wall motion imaging. *Circulation* 2007;115:1769–1776.
37. Kelle S, Chiribiri A, Vierecke J, et al. Long-term prognostic value of dobutamine stress CMR. *JACC Cardiovasc Imaging* 2011;4:161–172.
 38. Atkinson DJ, Burstein D, Edelman RR. First-pass cardiac perfusion: evaluation with ultrafast MR imaging. *Radiology* 1990;174:757–762.
 39. Gerber TC, Carr JJ, Arai AE, et al. Ionizing radiation in cardiac imaging: a science advisory from the American Heart Association Committee on Cardiac Imaging of the Council on Clinical Cardiology and Committee on Cardiovascular Imaging and Intervention of the Council on Cardiovascular Radiology and Intervention. *Circulation* 2009;119:1056–1065.
 40. Kellman P, Arai AE. Imaging sequences for first pass perfusion—a review. *J Cardiovasc Magn Reson* 2007;9:525–537.
 41. Iskandrian AE, Bateman TM, Belardinelli L, et al. Adenosine versus regadenoson comparative evaluation in myocardial perfusion imaging: results of the ADVANCE phase 3 multicenter international trial. *J Nucl Cardiol* 2007;14:645–658.
 42. Manka R, Jahnke C, Kozerke S, et al. Dynamic 3-dimensional stress cardiac magnetic resonance perfusion imaging detection of coronary artery disease and volumetry of myocardial hypoenhancement before and after coronary stenting. *J Am Coll Cardiol* 2011;57:437–444.
 43. Ishida N, Sakuma H, Motoyasu M, et al. Noninfarcted myocardium: correlation between dynamic first-pass contrast-enhanced myocardial MR imaging and quantitative coronary angiography. *Radiology* 2003;229:209–216.
 44. Schwitter J, Wacker CM, van Rossum AC, et al. MR-IMPACT: comparison of perfusion-cardiac magnetic resonance with single-photon emission computed tomography for the detection of coronary artery disease in a multicentre, multivendor, randomized trial. *Eur Heart J* 2008;29:480–489.
 45. Yong AS, Ng AC, Brieger D, Lowe HC, Ng MK, Krishanadas L. Three-dimensional and two-dimensional quantitative coronary angiography, and their prediction of reduced fractional flow reserve. *Eur Heart J* 2011;32:345–353.
 46. Costa MA, Shoemaker S, Futamatsu H, et al. Quantitative magnetic resonance perfusion imaging detects anatomic and physiologic coronary artery disease as measured by coronary angiography and fractional flow reserve. *J Am Coll Cardiol* 2007;50:514–522.
 47. Watkins S, McGeoch R, Lyne J, et al. Validation of magnetic resonance myocardial perfusion imaging with fractional flow reserve for the detection of significant coronary heart disease. *Circulation* 2009;120:2207–2213.
 48. Lockie T, Ishida M, Perera D, et al. High-resolution magnetic resonance myocardial perfusion imaging at 3.0-Tesla to detect hemodynamically significant coronary stenoses as determined by fractional flow reserve. *J Am Coll Cardiol* 2010;57:70–75.
 49. Klein C, Nagel E, Gebker R, et al. Magnetic resonance adenosine perfusion imaging in patients after coronary artery bypass graft surgery. *JACC Cardiovasc Imaging* 2009;2:437–445.
 50. Bernhardt P, Spiess J, Levenson B, et al. Combined assessment of myocardial perfusion and late gadolinium enhancement in patients after percutaneous coronary intervention or bypass grafts: a multicenter study of an integrated cardiovascular magnetic resonance protocol. *JACC Cardiovasc Imaging* 2009;2:1292–1300.
 51. Karamitsos TD, Arnold JR, Pegg TJ, et al. Tolerance and safety of adenosine stress perfusion cardiovascular magnetic resonance imaging in patients with severe coronary artery disease. *Int J Cardiovasc Imaging* 2009;25:277–283.
 52. Jerosch-Herold M. Quantification of myocardial perfusion by cardiovascular magnetic resonance. *J Cardiovasc Magn Reson* 2010;12:57.
 53. Utz W, Greiser A, Niendorf T, Dietz R, Schulz-Menger J. Single- or dual-bolus approach for the assessment of myocardial perfusion reserve in quantitative MR perfusion imaging. *Magn Reson Med* 2008;59:1373–1377.
 54. Patel AR, Antkowiak PF, Nandalur KR, et al. Assessment of advanced coronary artery disease: advantages of quantitative cardiac magnetic resonance perfusion analysis. *J Am Coll Cardiol* 2010;56:561–569.
 55. Araoz PA, Glockner JF, McGee KP, et al. 3 Tesla MR imaging provides improved contrast in first-pass myocardial perfusion imaging over a range of gadolinium doses. *J Cardiovasc Magn Reson* 2005;7:559–564.
 56. Cheng AS, Pegg TJ, Karamitsos TD, et al. Cardiovascular magnetic resonance perfusion imaging at 3-tesla for the detection of coronary artery disease: a comparison with 1.5-tesla. *J Am Coll Cardiol* 2007;49:2440–2449.
 57. Plein S, Schwitter J, Suerder D, Greenwood JP, Boesiger P, Kozerke S. k-Space and time sensitivity encoding-accelerated myocardial perfusion MR imaging at 3.0 T: comparison with 1.5 T. *Radiology* 2008;249:493–500.
 58. Plein S, Kozerke S, Suerder D, et al. High spatial resolution myocardial perfusion cardiac magnetic resonance for the detection of coronary artery disease. *Eur Heart J* 2008;29:2148–2155.
 59. Steel K, Broderick R, Gandla V, et al. Complementary prognostic values of stress myocardial perfusion and late gadolinium enhancement imaging by cardiac magnetic resonance in patients with known or suspected coronary artery disease. *Circulation* 2009;120:1390–1400.
 60. Ingkanisorn WP, Kwong RY, Bohme NS, et al. Prognosis of negative adenosine stress magnetic resonance in patients presenting to an emergency department with chest pain. *J Am Coll Cardiol* 2006;47:1427–1432.
 61. Wagner A, Mahrholdt H, Holly TA, et al. Contrast-enhanced MRI and routine single photon emission computed tomography (SPECT) perfusion imaging for detection of subendocardial myocardial infarcts: an imaging study. *Lancet* 2003;361:374–379.
 62. Kim RJ, Albert TS, Wible JH, et al. Performance of delayed-enhancement magnetic resonance imaging with gadoversetamide contrast for the detection and assessment of myocardial infarction: an international, multicenter, double-blinded, randomized trial. *Circulation* 2008;117:629–637.
 63. Klem I, Heitner JF, Shah DJ, et al. Improved detection of coronary artery disease by stress perfusion cardiovascular magnetic resonance with the use of delayed enhancement infarction imaging. *J Am Coll Cardiol* 2006;47:1630–1638.
 64. Cury RC, Shash K, Nagurny JT, et al. Cardiac magnetic resonance with T2-weighted imaging improves detection of patients with acute coronary syndrome in the emergency department. *Circulation* 2008;118:837–844.
 65. Friedrich MG. Myocardial edema—a new clinical entity? *Nat Rev Cardiol* 2010;7:292–296.
 66. McNamara MT, Higgins CB, Ehman RL, Revel D, Sievers R, Brasch RC. Acute myocardial ischemia: magnetic resonance contrast enhancement with gadolinium-DTPA. *Radiology* 1984;153:157–163.
 67. Eichstaedt HW, Felix R, Dougherty FC, Langer M, Rutsch W, Schmutzler H. Magnetic resonance imaging (MRI) in different stages of myocardial infarction using the contrast agent gadolinium-DTPA. *Clin Cardiol* 1986;9:527–535.
 68. Kim RJ, Chen EL, Lima JA, Judd RM. Myocardial Gd-DTPA kinetics determine MRI contrast enhancement and reflect the extent and severity of myocardial injury after acute reperfused infarction. *Circulation* 1996;94:3318–3326.
 69. Kim RJ, Fieno DS, Parrish TB, et al. Relationship of MRI delayed contrast enhancement to irreversible injury, infarct age, and contractile function. *Circulation* 1999;100:1992–2002.
 70. Simonetti OP, Kim RJ, Fieno DS, et al. An improved MR imaging technique for the visualization of myocardial infarction. *Radiology* 2001;218:215–223.
 71. Kino A, Zuehlsdorff S, Sheehan JJ, et al. Three-dimensional phase-sensitive inversion-recovery turbo FLASH sequence for the evaluation of left ventricular myocardial scar. *AJR Am J Roentgenol* 2009;193:W381–W388.
 72. Ledesma-Carbayo MJ, Kellman P, Hsu LY, Arai AE, McVeigh ER. Motion corrected free-breathing delayed-enhancement imaging of myocardial infarction using nonrigid registration. *J Magn Reson Imaging* 2007;26:184–190.
 73. Mewton N, Liu CY, Croisille P, Bluemke D, Lima JA. Assessment of myocardial fibrosis with cardiovascular magnetic resonance. *J Am Coll Cardiol* 2011;57:891–903.
 74. Ibrahim T, Bulow HP, Hackl T, et al. Diagnostic value of contrast-enhanced magnetic resonance imaging and single-photon emission computed tomography for detection of myocardial

- necrosis early after acute myocardial infarction. *J Am Coll Cardiol* 2007;49:208–216.
75. Klein C, Nekolla SG, Bengel FM, et al. Assessment of myocardial viability with contrast-enhanced magnetic resonance imaging: comparison with positron emission tomography. *Circulation* 2002;105:162–167.
 76. Reimer KA, Lowe JE, Rasmussen MM, Jennings RB. The wave-front phenomenon of ischemic cell death. 1. Myocardial infarct size vs duration of coronary occlusion in dogs. *Circulation* 1977;56:786–794.
 77. Abdel-Aty H, Boye P, Zagrosek A, et al. Diagnostic performance of cardiovascular magnetic resonance in patients with suspected acute myocarditis: comparison of different approaches. *J Am Coll Cardiol* 2005;45:1815–1822.
 78. Bohl S, Wassmuth R, Abdel-Aty H, et al. Delayed enhancement cardiac magnetic resonance imaging reveals typical patterns of myocardial injury in patients with various forms of non-ischemic heart disease. *Int J Cardiovasc Imaging* 2008;24:597–607.
 79. Mahrholdt H, Wagner A, Parker M, et al. Relationship of contractile function to transmural extent of infarction in patients with chronic coronary artery disease. *J Am Coll Cardiol* 2003;42:505–512.
 80. Kwong RY, Chan AK, Brown KA, et al. Impact of unrecognized myocardial scar detected by cardiac magnetic resonance imaging on event-free survival in patients presenting with signs or symptoms of coronary artery disease. *Circulation* 2006;113:2733–2743.
 81. Ricciardi MJ, Wu E, Davidson CJ, et al. Visualization of discrete microinfarction after percutaneous coronary intervention associated with mild creatine kinase-MB elevation. *Circulation* 2001;103:2780–2783.
 82. Kumar A, Abdel-Aty H, Kriedemann I, et al. Contrast-enhanced cardiovascular magnetic resonance imaging of right ventricular infarction. *J Am Coll Cardiol* 2006;48:1969–1976.
 83. Larose E, Ganz P, Reynolds HG, et al. Right ventricular dysfunction assessed by cardiovascular magnetic resonance imaging predicts poor prognosis late after myocardial infarction. *J Am Coll Cardiol* 2007;49:855–862.
 84. Tanimoto T, Imanishi T, Kitabata H, et al. Prevalence and clinical significance of papillary muscle infarction detected by late gadolinium-enhanced magnetic resonance imaging in patients with ST-segment elevation myocardial infarction. *Circulation* 2010;122:2281–2287.
 85. Okayama S, Uemura S, Soeda T, et al. Clinical significance of papillary muscle late enhancement detected via cardiac magnetic resonance imaging in patients with single old myocardial infarction. *Int J Cardiol* 2011;146:73–79.
 86. Thiel H, Kappl MJ, Conradi S, Niebauer J, Hambrecht R, Schuler G. Reproducibility of chronic and acute infarct size measurement by delayed enhancement-magnetic resonance imaging. *J Am Coll Cardiol* 2006;47:1641–1645.
 87. Kellman P, Hernando D, Shah S, et al. Multiecho dixon fat and water separation method for detecting fibrofatty infiltration in the myocardium. *Magn Reson Med* 2009;61:215–221.
 88. Goldfarb JW, Roth M, Han J. Myocardial fat deposition after left ventricular myocardial infarction: assessment by using MR water-fat separation imaging. *Radiology* 2009;253:65–73.
 89. Lockie T, Nagel E, Redwood S, Plein S. Use of cardiovascular magnetic resonance imaging in acute coronary syndromes. *Circulation* 2009;119:1671–1681.
 90. Flett AS, Westwood MA, Davies LC, Mathur A, Moon JC. The prognostic implications of cardiovascular magnetic resonance. *Circ Cardiovasc Imaging* 2009;2:243–250.
 91. Abdel-Aty H, Simonetti O, Friedrich MG. T2-weighted cardiovascular magnetic resonance imaging. *J Magn Reson Imaging* 2007;26:452–459.
 92. Eitel I, Friedrich MG. T2-weighted cardiovascular magnetic resonance in acute cardiac disease. *J Cardiovasc Magn Reson* 2011;13:13.
 93. Higgins CB, Herfkens R, Lipton MJ, et al. Nuclear magnetic resonance imaging of acute myocardial infarction in dogs: alterations in magnetic relaxation times. *Am J Cardiol* 1983;52:184–188.
 94. Simonetti OP, Finn JP, White RD, Laub G, Henry DA. "Black blood" T2-weighted inversion-recovery MR imaging of the heart. *Radiology* 1996;199:49–57.
 95. Kellman P, Aletras AH, Mancini C, McVeigh ER, Arai AE. T2-prepared SSFP improves diagnostic confidence in edema imaging in acute myocardial infarction compared to turbo spin echo. *Magn Reson Med* 2007;57:891–897.
 96. Abdel-Aty H, Cocker M, Strohm O, Filipchuk N, Friedrich MG. Abnormalities in T2-weighted cardiovascular magnetic resonance images of hypertrophic cardiomyopathy: regional distribution and relation to late gadolinium enhancement and severity of hypertrophy. *J Magn Reson Imaging* 2008;28:242–245.
 97. Abdel-Aty H, Cocker M, Meek C, Tyberg JV, Friedrich MG. Edema as a very early marker for acute myocardial ischemia: a cardiovascular magnetic resonance study. *J Am Coll Cardiol* 2009;53:1194–1201.
 98. Schulz-Menger J, Gross M, Messroghli D, Uhlich F, Dietz R, Friedrich MG. Cardiovascular magnetic resonance of acute myocardial infarction at a very early stage. *J Am Coll Cardiol* 2003;42:513–518.
 99. Friedrich MG, Abdel-Aty H, Taylor A, Schulz-Menger J, Messroghli D, Dietz R. The salvaged area at risk in reperfused acute myocardial infarction as visualized by cardiovascular magnetic resonance. *J Am Coll Cardiol* 2008;51:1581–1587.
 100. Francone M, Buccarelli-Ducci C, Carbone I, et al. Impact of primary coronary angioplasty delay on myocardial salvage, infarct size, and microvascular damage in patients with ST-segment elevation myocardial infarction: insight from cardiovascular magnetic resonance. *J Am Coll Cardiol* 2009;54:2145–2153.
 101. Abdel-Aty H, Zagrosek A, Schulz-Menger J, et al. Delayed enhancement and T2-weighted cardiovascular magnetic resonance imaging differentiate acute from chronic myocardial infarction. *Circulation* 2004;109:2411–2416.
 102. Nilsson JC, Nielsen G, Groenning BA, et al. Sustained postinfarction myocardial oedema in humans visualised by magnetic resonance imaging. *Heart* 2001;85:639–642.
 103. Weinsaft JW, Kim HW, Shah DJ, et al. Detection of left ventricular thrombus by delayed-enhancement cardiovascular magnetic resonance prevalence and markers in patients with systolic dysfunction. *J Am Coll Cardiol* 2008;52:148–157.
 104. Mollet NR, Dymarkowski S, Volders W, et al. Visualization of ventricular thrombi with contrast-enhanced magnetic resonance imaging in patients with ischemic heart disease. *Circulation* 2002;106:2873–2876.
 105. Srichai MB, Junor C, Rodriguez LL, et al. Clinical, imaging, and pathological characteristics of left ventricular thrombus: a comparison of contrast-enhanced magnetic resonance imaging, transthoracic echocardiography, and transesophageal echocardiography with surgical or pathological validation. *Am Heart J* 2006;152:75–84.
 106. Baer FM, Theissen P, Schneider CA, et al. Dobutamine magnetic resonance imaging predicts contractile recovery of chronically dysfunctional myocardium after successful revascularization. *J Am Coll Cardiol* 1998;31:1040–1048.
 107. Baer FM, Smolarz K, Jungehulsing M, et al. Chronic myocardial infarction: assessment of morphology, function, and perfusion by gradient echo magnetic resonance imaging and 99mTc-methoxyisobutyl-isonitrile SPECT. *Am Heart J* 1992;123:636–645.
 108. Bove CM, DiMaria JM, Voros S, Conaway MR, Kramer CM. Dobutamine response and myocardial infarct transmurality: functional improvement after coronary artery bypass grafting—initial experience. *Radiology* 2006;240:835–841.
 109. Kim RJ, Wu E, Rafael A, et al. The use of contrast-enhanced magnetic resonance imaging to identify reversible myocardial dysfunction. *N Engl J Med* 2000;343:1445–1453.
 110. Selvanayagam JB, Kardos A, Francis JM, et al. Value of delayed-enhancement cardiovascular magnetic resonance imaging in predicting myocardial viability after surgical revascularization. *Circulation* 2004;110:1535–1541.
 111. Wellnhofer E, Olariu A, Klein C, et al. Magnetic resonance low-dose dobutamine test is superior to SCAR quantification for the prediction of functional recovery. *Circulation* 2004;109:2172–2174.
 112. Kirschbaum SW, Rossi A, van Domburg RT, et al. Contractile reserve in segments with nontransmural infarction in chronic dysfunctional myocardium using low-dose dobutamine CMR. *JACC Cardiovasc Imaging* 2010;3:614–622.

113. Ichikawa Y, Sakuma H, Suzawa N, et al. Late gadolinium-enhanced magnetic resonance imaging in acute and chronic myocardial infarction. Improved prediction of regional myocardial contraction in the chronic state by measuring thickness of nonenhanced myocardium. *J Am Coll Cardiol* 2005;45:901–909.
114. Glaveckaite S, Valeviciene N, Palionis D, et al. Value of scar imaging and inotropic reserve combination for the prediction of segmental and global left ventricular functional recovery after revascularisation. *J Cardiovasc Magn Reson* 2011;13:35.
115. Kwong RY, Sattar H, Wu H, et al. Incidence and prognostic implication of unrecognized myocardial scar characterized by cardiac magnetic resonance in diabetic patients without clinical evidence of myocardial infarction. *Circulation* 2008;118:1011–1020.
116. Roes SD, Kelle S, Kaandorp TA, et al. Comparison of myocardial infarct size assessed with contrast-enhanced magnetic resonance imaging and left ventricular function and volumes to predict mortality in patients with healed myocardial infarction. *Am J Cardiol* 2007;100:930–936.
117. Kwon DH, Hally CM, Carrigan TP, et al. Extent of left ventricular scar predicts outcomes in ischemic cardiomyopathy patients with significantly reduced systolic function: a delayed hyperenhancement cardiac magnetic resonance study. *JACC Cardiovasc Imaging* 2009;2:34–44.
118. Boye P, Abdel-Aty H, Zacharowsky U, et al. Prediction of life-threatening arrhythmic events in patients with chronic myocardial infarction by contrast-enhanced CMR. *JACC Cardiovasc Imaging* 2011;4:871–879.
119. Roes SD, Borleffs CJ, van der Geest RJ, et al. Infarct tissue heterogeneity assessed with contrast-enhanced MRI predicts spontaneous ventricular arrhythmia in patients with ischemic cardiomyopathy and implantable cardioverter-defibrillator. *Circ Cardiovasc Imaging* 2009;2:183–190.
120. Epstein AE, DiMarco JP, Ellenbogen KA, et al. ACC/AHA/HRS 2008 Guidelines for device-based therapy of cardiac rhythm abnormalities: a report of the American College of Cardiology/American Heart Association Task Force on Practice Guidelines (writing committee to revise the ACC/AHA/NASPE 2002 guideline update for implantation of cardiac pacemakers and antiarrhythmia devices): developed in collaboration with the American Association for Thoracic Surgery and Society of Thoracic Surgeons. *Circulation* 2008;117:e350–408.
121. Schelbert EB, Hsu LY, Anderson SA, et al. Late gadolinium-enhancement cardiac magnetic resonance identifies postinfarction myocardial fibrosis and the border zone at the near cellular level in ex vivo rat heart. *Circ Cardiovasc Imaging* 2010;3:743–752.
122. Eitel I, Desch S, Fuernau G, et al. Prognostic significance and determinants of myocardial salvage assessed by cardiovascular magnetic resonance in acute reperfused myocardial infarction. *J Am Coll Cardiol* 2010;55:2470–2479.
123. Raman SV, Simonetti OP, Winner MW III, et al. Cardiac magnetic resonance with edema imaging identifies myocardium at risk and predicts worse outcome in patients with non-ST-segment elevation acute coronary syndrome. *J Am Coll Cardiol* 2010;55:2480–2488.
124. Ganame J, Messalli G, Dymarkowski S, et al. Impact of myocardial haemorrhage on left ventricular function and remodelling in patients with reperfused acute myocardial infarction. *Eur Heart J* 2009;30:1440–1449.
125. Mather AN, Fairbairn TA, Ball SG, Greenwood JP, Plein S. Reperfusion haemorrhage as determined by cardiovascular MRI is a predictor of adverse left ventricular remodelling and markers of late arrhythmic risk. *Heart* 2011;97:453–459.
126. Bekkers SC, Yazdani SK, Virmani R, Waltenberger J. Microvascular obstruction: underlying pathophysiology and clinical diagnosis. *J Am Coll Cardiol* 2010;55:1649–1660.
127. de Waha S, Desch S, Eitel I, et al. Impact of early vs. late microvascular obstruction assessed by magnetic resonance imaging on long-term outcome after ST-elevation myocardial infarction: a comparison with traditional prognostic markers. *Eur Heart J* 2010;31:2660–2668.
128. Nijveldt R, Beek AM, Hirsch A, et al. Functional recovery after acute myocardial infarction: comparison between angiography, electrocardiography, and cardiovascular magnetic resonance measures of microvascular injury. *J Am Coll Cardiol* 2008;52:181–189.
129. Hombach V, Grebe O, Merkle N, et al. Sequelae of acute myocardial infarction regarding cardiac structure and function and their prognostic significance as assessed by magnetic resonance imaging. *Eur Heart J* 2005;26:549–557.
130. Larson DM, Menssen KM, Sharkey SW, et al. "False-positive" cardiac catheterization laboratory activation among patients with suspected ST-segment elevation myocardial infarction. *JAMA* 2007;298:2754–2760.
131. Flett AS, Hasleton J, Cook C, et al. Evaluation of techniques for the quantification of myocardial scar of differing etiology using cardiac magnetic resonance. *JACC Cardiovasc Imaging* 2011;4:150–156.
132. Mather AN, Fairbairn TA, Artis NJ, Greenwood JP, Plein S. Timing of cardiovascular MR imaging after acute myocardial infarction: effect on estimates of infarct characteristics and prediction of late ventricular remodeling. *Radiology* 2011;261:116–126.
133. Wince WB, Kim RJ. Molecular imaging: T2-weighted CMR of the area at risk—a risky business? *Nat Rev Cardiol* 2010;7:547–549.
134. Verhaert D, Thavendiranathan P, Giri S, et al. Direct t2 quantification of myocardial edema in acute ischemic injury. *JACC Cardiovasc Imaging* 2011;4:269–278.
135. Ogawa S, Lee TM, Kay AR, Tank DW. Brain magnetic resonance imaging with contrast dependent on blood oxygenation. *Proc Natl Acad Sci U S A* 1990;87:9868–9872.
136. Friedrich MG, Niendorf T, Schulz-Menger J, Gross CM, Dietz R. Blood oxygen level-dependent magnetic resonance imaging in patients with stress-induced angina. *Circulation* 2003;108:2219–2223.
137. Jahnke C, Gebker R, Manka R, Schnackenburg B, Fleck E, Paetsch I. Navigator-gated 3D blood oxygen level-dependent CMR at 3.0-T for detection of stress-induced myocardial ischemic reactions. *JACC Cardiovasc Imaging* 2010;3:375–384.
138. Karamitsos TD, Leccisotti L, Arnold JR, et al. Relationship between regional myocardial oxygenation and perfusion in patients with coronary artery disease: insights from cardiovascular magnetic resonance and positron emission tomography. *Circ Cardiovasc Imaging* 2010;3:32–40.
139. Stuber M, Weiss RG. Coronary magnetic resonance angiography. *J Magn Reson Imaging* 2007;26:219–234.
140. Kato S, Kitagawa K, Ishida N, et al. Assessment of coronary artery disease using magnetic resonance coronary angiography: a national multicenter trial. *J Am Coll Cardiol* 2010;56:983–991.
141. Hamdan A, Asbach P, Wellnhofer E, et al. A prospective study for comparison of MR and CT imaging for detection of coronary artery stenosis. *JACC Cardiovasc Imaging* 2011;4:50–61.
142. Botnar RM, Stuber M, Kissinger KV, Kim WY, Spuentrup E, Manning WJ. Noninvasive coronary vessel wall and plaque imaging with magnetic resonance imaging. *Circulation* 2000;102:2582–2587.
143. Hays AG, Hirsch GA, Kelle S, Gerstenblith G, Weiss RG, Stuber M. Noninvasive visualization of coronary artery endothelial function in healthy subjects and in patients with coronary artery disease. *J Am Coll Cardiol* 2010;56:1657–1665.
144. Ibrahim T, Makowski MR, Jankauskas A, et al. Serial contrast-enhanced cardiac magnetic resonance imaging demonstrates regression of hyperenhancement within the coronary artery wall in patients after acute myocardial infarction. *JACC Cardiovasc Imaging* 2009;2:580–588.
145. Lin K, Lloyd-Jones DM, Liu Y, Bi X, Li D, Carr JC. Noninvasive evaluation of coronary distensibility in older adults: a feasibility study with MR angiography. *Radiology* 2011;261:771–778.
146. Makowski MR, Wiethoff AJ, Blume U, et al. Assessment of atherosclerotic plaque burden with an elastin-specific magnetic resonance contrast agent. *Nat Med* 2011;17:383–388.
147. von Knobelsdorff-Brenkenhoff F, Frauenrath T, Prothmann M, et al. Cardiac chamber quantification using magnetic resonance imaging at 7 Tesla—pilot study. *Eur Radiol* 2010;20:2844–2852.
148. van Elderen SG, Versluis MJ, Westenberg JJ, et al. Right coronary MR angiography at 7 T: a direct quantitative and qualitative comparison with 3 T in young healthy volunteers. *Radiology* 2010;257:254–259.
149. Wu MT, Su MY, Huang YL, et al. Sequential changes of myocardial microstructure in patients postmyocardial infarction by diffusion-tensor cardiac MR: correlation with left ventricular structure and function. *Circ Cardiovasc Imaging* 2009;2:32–40.
150. Sosnovik DE, Wang R, Dai G, Reese TG, Wedeen VJ. Diffusion MR tractography of the heart. *J Cardiovasc Magn Reson* 2009;11:47.